12-4-2014 12:00 AM

Enhanced Dechlorination of 1,2-Dichloroethane by Coupled Nano Iron-Dithionite Treatment

Ariel Nunez Garcia, *The University of Western Ontario*

Supervisor: Denis M. O'Carroll, *The University of Western Ontario*

A thesis submitted in partial fulfillment of the requirements for the Master of Engineering Science degree in Civil and Environmental Engineering

ENHANCED DECHLORINATION OF 1,2-DICHLOROETHANE BY COUPLED NANO IRON-DITHIONITE TREATMENT

(Thesis Format: Integrated-Article)

By

Ariel Núñez García

Graduate Program in Engineering Science

Department of Civil and Environmental Engineering

A thesis submitted in partial fulfillment of the requirements for the degree of

Master of Engineering Science

The School of Graduate and Postdoctoral Studies

The University of Western Ontario

London, Ontario, Canada

Abstract

1,2-dichloroethane (1,2-DCA) is a chlorinated solvent classified as a probable human carcinogen. Due to its extensive industrial applications, widespread contamination and recalcitrance towards abiotic dechlorination, 1,2-DCA remains a challenging compound for the remediation community and one of the great research interests. Batch experiments combining bimetallic or monometallic nZVI (stabilized or non-stabilized) with sodium dithionite were conducted for the degradation of 1,2-DCA. These experiments have yielded up to 92 % degradation of the initial 1,2-DCA concentration over the course of a year. Observed pseudo-first order rate constants (k_{obs}) range from 3.8 x 10^{-3} to 7.8 x 10^{-3} day^{-1}. Degradation was also achieved using magnetite and iron sulfide as the metal surface, with kobs values of 6.2 x 10^{-3} and 4.7 x 10^{-3} day^{-1}, respectively. Characterization analysis of the nZVI/dithionite nanoparticles shows that zero valent iron as such remains in solution after more than one year of reactivity and that iron sulfide is formed in solution. This novel treatment represents the first nZVI-based formulation to achieve nearly complete degradation of 1,2-DCA.

Keywords: Nano-scale zero valent iron, nZVI, sodium dithionite, 1,2-DCA, reductant

Co-Authorship Statement

The candidate conducted all the laboratory experiments; collected, interpreted and analyzed the experimental data under the close guidance and supervision of Dr. O'Carroll and Dr. Boparai. The candidate wrote the manuscript draft of the following chapter:

Chapter 3: Enhanced dechlorination of 1,2-dichloroethane by coupled nano iron - dithionite treatment.

By Ariel Núñez García, Hardiljeet K. Boparai and Denis M. O'Carroll

Contributions:

Ariel Núñez García:	performed all the experiments, collected and interpreted experimental results, and wrote the draft of the paper.
Hardiljeet K. Boparai:	initiated the research topics, supervised laboratory tests, assisted in data interpretation, and reviewed/revised the draft chapter.
Denis M. O'Carroll:	initiated the research topics, supervised laboratory tests, assisted in data interpretation, and reviewed/revised the draft chapter.

Acknowledgments

First, I thank and praise God for giving me the strength and perseverance to finish this work.

I would like to thank my supervisor, Dr. Denis M. O'Carroll, for his support and guidance. I have greatly enjoyed the last two years working with him. Special thanks to Dr. Hardiljeet Boparai for the endless hours of discussion regarding my experiments and data analysis. Her guidance, inputs and dedication were essential for the completion of this research work.

I want to express my gratitude to all RESTORE members for providing a welcoming atmosphere. Special thanks to Ahmed Chowdhury and Jorge Gabayet for all their help and advice. I want to thank Dr. O'Carroll, Dr. Gerhard and Dr. Robinson for leading the RESTORE weekly group meetings. The inputs and feedbacks they provided for my presentations have made me a better researcher. I also want to thank Dr. Herrera and members of the LDAN research team for their help and technical advice.

Finally, I want to thank my family and friends. Their support and encouragement has made this achievement possible.

Table of Contents

List of Tables

List of Figures

Chapter 1

1. Introduction

1.1. Background

Improper handling, storage and disposal of hazardous wastes over the last one hundred years have caused extensive contamination to the environment, posing threats to public health and ecological systems. Hazardous waste site remediation also represents a huge economic burden to local municipalities and federal agencies. Estimates made in the 1990's predicted that remediation costs in the U.S. over the next three decades will be approximately $750 billion US (Soesilo and Wilson, 1997). As one of the most complex environmental issues nowadays, the large number of contaminated sites throughout North America demands the development of new cost-effective technologies for their remediation. In response, a variety of innovative remedial technologies have been developed over the years. These include chemical flushing, in-situ chemical oxidation and reduction, gas and steam treatment and thermal treatment technologies (Soga et al., 2004). Even though significant progress has been made over the last two decades, existing remediation methods are rarely able to achieve clean-up goals, hence the need to develop more efficient technologies for site remediation (O'Carroll et al., 2013). Amongst the emerging technologies, nano zero valent iron (nZVI) stands out as one of the most promising due to its high reactivity.

Zero-valent iron is an excellent reductant with a standard reduction potential of -0.44 V (Equation 1.1), and its electron-donating properties have received a lot of attention from researchers since the mid-1990s. Micro scale zero-valent iron (mZVI) is effective for the treatment of many environmental contaminants, including chlorinated alkanes and alkenes,

polychlorinated biphenyls (PCBs), chlorinated pesticides, nitro aromatic compounds, and metals among others (O'Carroll et al., 2013).

$Fe^{2+} + 2e^- \rightarrow Fe^0$ ($E^0 = -0.44$ V) Eq. 1.1

To increase the reactivity of ZVI, nano-scale particles doped with noble metals (e.g., Ni, Pd) are frequently employed. Even though rapid dechlorination of chlorinated ethenes and ethanes has been reported using monometallic and bimetallic (Pd/Fe) iron nanoparticles, nZVI is unreactive towards 1,2-Dichloroethane (1,2-DCA), to the point that its application to degrade this contaminant is currently impractical (Lien and Zhang, 2001, Lien and Zhang, 2005, Song and Carraway, 2005). Studies have suggested that effective degradation of 1,2-DCA by a metal requires strong reducing conditions, with the reducing metal having a redox potential lower than -0.8 V (Huang et al., 2011). Therefore, an effective treatment for the degradation of 1,2-DCA involving nZVI would necessitate the inclusion of a secondary reductant.

Sodium dithionite is a well-known reductant and is widely used in industry and remediation field. The use of dithionite in the field for the reduction of redox sensitive contaminants is a proven technology, with reducing conditions remaining even after several years of its initial injection (Naftz et al., 2002). Based on its wide acceptance and efficiency for remediation applications, a combination of nZVI and sodium dithionite is hypothesized to offer a practical treatment for the creation of the strong reducing conditions necessary to degrade 1,2-DCA.

1.2. Objectives

The objectives of this research work are to develop an nZVI/Dithionite treatment for the effective degradation of 1,2-Dichloroethane and evaluate the effect of dithionite on the morphology, reactivity and longevity of nZVI.

1.3. Thesis Outline

This thesis is presented as an "Integrated Article Format". Below is an outline of the content of each chapter:

Chapter 1: introduction to the challenge of hazardous waste sites, nZVI technology, 1,2-DCA and presentation of research objectives.

Chapter 2: description of nZVI, background and review of previous research on 1,2-DCA dechlorination.

Chapter 3: literature review, methodologies and discussion of experimental results.

Chapter 4: conclusion and recommendations.

1.4. References

Huang, C. C., S. L. Lo, S. M. Tsai and H. L. Lien (2011). "Catalytic hydrodechlorination of 1,2-dichloroethane using copper nanoparticles under reduction conditions of sodium borohydride." Journal of Environmental Monitoring **13**(9): 2406-2412.

Lien, H. L. and W. X. Zhang (2001). "Nanoscale iron particles for complete reduction of chlorinated ethenes." Colloids and Surfaces a-Physicochemical and Engineering Aspects **191**(1-2): 97-105.

Lien, H. L. and W. X. Zhang (2005). "Hydrodechlorination of chlorinated ethanes by nanoscale Pd/Fe bimetallic particles." Journal of Environmental Engineering-Asce **131**(1): 4-10.

Naftz, D. L., S. J. Morrison, J. A. Davis and C. C. Fuller (2002). Handbook of groundwater remediation using permeable reactive barriers : applications to radionuclides, trace metals, and nutrients. San Diego, CA, San Diego, CA: Academic Press, c2002.

O'Carroll, D., B. Sleep, M. Krol, H. Boparai and C. Kocur (2013). "Nanoscale zero valent iron and bimetallic particles for contaminated site remediation." Advances in Water Resources **51**: 104-122.

Soesilo, J. A. and S. R. Wilson (1997). Site Remediation Planning and Management. Boca Raton, FL, Lewis Publishers.

Soga, K., J. W. E. Page and T. H. Illangasekare (2004). "A review of NAPL source zone remediation efficiency and the mass flux approach." Journal of Hazardous Materials **110**(1-3): 13-27.

Song, H. and E. R. Carraway (2005). "Reduction of chlorinated ethanes by nanosized zero-valent iron: Kinetics, pathways, and effects of reaction conditions." Environmental Science & Technology **39**(16): 6237-6245.

Chapter 2

2. Literature Review

2.1. Introduction

One of the most common contaminants at brownfield and industrialized sites are chlorinated solvents, a particularly recalcitrant class of non-aqueous phase liquids (NAPLs) (O'Carroll et al., 2013). Of these compounds, chlorinated ethanes and ethenes are one of the most commonly found in contaminated groundwater (Song and Carraway, 2005). Their ubiquity is due to their extensive industrial applications as degreasing agents, detergents, paint removers, dyes, solvents, and intermediates in the manufacture of other chemicals. These compounds are suspected or known human carcinogens and their resistance to biotic or abiotic transformations has made them prevalent groundwater contaminants (Song and Carraway, 2005).

Micro-scale zero valent iron (mZVI) has been used for the dechlorination of chlorinated compounds since the mid-1990s. Due to its relatively large size, mZVI has been mainly employed in permeable reactive barriers (PRBs) for in-situ remediation, and its application is limited due of engineering constraints. PRBs have a high construction cost (especially for deep aquifers), a large amount of iron powder is necessary, even for small installations, and relocation or major modifications of the PRB structure are impractical (Li et al., 2006). To address these issues, Wang and Zhang (1997) reported a method for synthesizing ZVI nanoparticles. These nanoparticles are more reactive than commercial iron powders, likely due to their higher specific surface area and surface reactivity. The dechlorination of chlorinated compounds by ZVI particles is a surface-mediated process, as such increasing specific surface area (by reducing particle size) will increase the dechlorination rate (He and Zhao, 2005). Another advantage of reducing the size of Fe^0 is the possibility of directly injecting the particles into the subsurface,

overcoming the limitations encountered with mZVI. For these reasons, nanoscale zero-valent iron (nZVI) has become an attractive option for in situ remediation.

2.2. Nanoscale Zero Valent Iron

nZVI has a core-shell structure with a core composed of zero-valent iron (Fe^0) and a shell largely made of iron oxides (likely in the form of FeO) (Sun et al., 2006). The average size of nZVI rages from 1 to 100 nm and the BET specific surface area has been reported to be 10 - 50 m^2/g (Wang and Zhang, 1997, Sun et al., 2006, Yan et al., 2013). In comparison, commercially available fine iron powder has a specific surface area of about 0.9 m^2/g (Wang and Zhang, 1997). In aqueous solution, nZVI reacts with water and dissolved oxygen (Equations 2.1 – 2.2), yielding hydroxides, hydrogen gas (H_2) and ferrous iron (Li et al., 2006, Sun et al., 2006).

$$Fe^0 + 2H_2O \rightarrow Fe^{2+} + H_2 + 2OH^- \qquad \text{Eq. 2.1}$$

$$2Fe^0 + O_2 + 2H_2O \rightarrow 2Fe^{2+} + 4OH^- \qquad \text{Eq. 2.2}$$

Ferrous iron can be further oxidized to ferric iron (Equation 2.3) and react with hydroxides and water to form iron (oxy)hydroxides (Equations 2.4 – 2.5). These forms of iron are responsible for the core-shell structure of nZVI by precipitating onto the iron surface, forming an outer iron (oxy)hydroxide layer and preserving the reduced α-Fe in the core (O'Carroll et al., 2013).

$$4Fe^{2+} + 4H^+ + O_2 \rightarrow 4Fe^{3+} + 2H_2O \qquad \text{Eq. 2.3}$$

$$Fe^{3+} + 3OH^- \rightarrow Fe(OH)_3 \qquad \text{Eq. 2.4}$$

$$Fe^{3+} + 2H_2O \rightarrow FeOOH + 3H^+ \qquad \text{Eq. 2.5}$$

2.2.1. Synthesis

Nano-scale zero-valent iron is commonly synthesized by reduction of ferric iron [Fe(III)] (or ferrous iron [Fe(II)]) using sodium borohydride and an iron precursor. This method is simple and requires only two reagents; an iron precursor (ferric chloride hexahydrate, $FeCl_3.6H_2O$, or ferrous sulphate heptahydrate, $FeSO_4.7H_2O$) and sodium borohydride ($NaBH_4$). For example, synthesis of nZVI using $FeCl_3.6H_2O$ occurs according to Equation 2.6 (Sun et al., 2006, Zhang and Elliott, 2006):

$$4Fe^{3+} + 3BH^{-4} + 9H_2O \rightarrow 4Fe^0 + 3H_2B^{-3} + 12H^+ + 6H_2 \qquad \text{Eq. 2.6}$$

Ferrous sulphate heptahydrate is preferred over its chloride counterpart because it allows for an easier monitoring of chloride production and it eliminates health and safety concerns associated with the use of a ferric chloride salt. Besides, because of its lower oxidation state, reduction of $FeSO_4.7H_2O$ requires less borohydride than needed for $FeCl_3.6H_2O$ reduction (Equation 2.7), making the process more economic (Zhang and Elliott, 2006).

$$2Fe^{2+} + BH_4^- + 3H_2O \rightarrow 2Fe^0 + H_2BO_3^- + 4H^+ + 2H_2 \qquad \text{Eq. 2.7}$$

2.2.2. Bimetallic and Stabilized nZVI

To enhance the reactivity of nZVI, Wang and Zhang (1997) also reported a method for synthesizing bimetallic iron nanoparticles. These nanoparticles (e.g., Pd/Fe, Ni/Fe) are often incorporated into the reaction because they can achieve higher degradation rates than monometallic nZVI and prevent the formation of toxic byproducts (Li et al., 2006). The second noble metal acts as a catalyst and enhances the nano iron activation and use of H_2. This process increases its dechlorination efficiency because now the electrons used to reduce water to H_2 can

also be used to reduce the chlorinated compound rather than being lost (Liu et al., 2005). This process is illustrated in Figure 2.1.

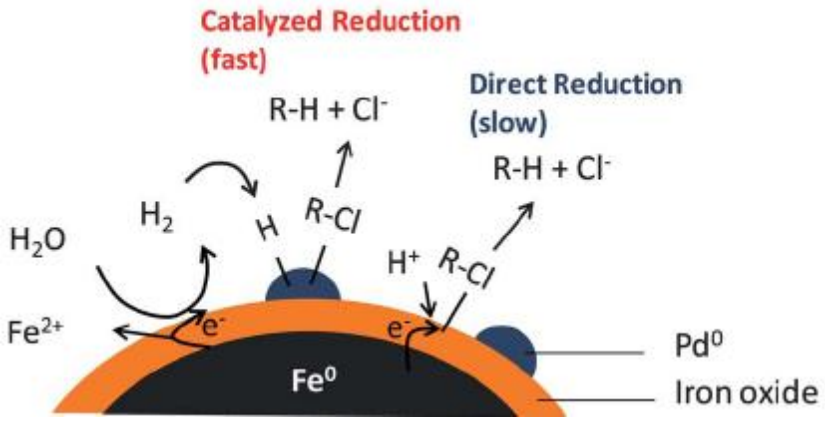

Figure 2.1 Monometallic and bimetallic nZVI reactivity with chlorinated compounds (Yan et al., 2013)

Palladium is the most common noble metal used for reductive dehalogenation and can be added through a water-based approach in which iron reduces palladium and this in turn is deposited onto the iron surface (Equation 2.8) (O'Carroll et al., 2013):

$$Pd^{2+} + Fe^{0} \rightarrow Pd^{0} + Fe^{2+} \qquad \text{Eq. 2.8}$$

ZVI nanoparticles rapidly agglomerate to form larger aggregates due to van der Waals and magnetic forces (He and Zhao, 2005, Phenrat et al., 2007). This phenomenon hinders their mobility and greatly reduces their reactive surface area. To prevent agglomeration and decrease particle size, different stabilizers have been proposed. These stabilizers include hydrophilic carbon and poly(acrylic acid) (PAA) (Schrick et al., 2004), starch (He and Zhao, 2005), carboxymethyl cellulose (CMC) (He and Zhao, 2007), guar gum (Tiraferri et al., 2008), triblock copolymer (PMAA-PMMA-PSS) and SDBS surfactants (Saleh et al., 2007). The stabilization mechanism can be through electrostatic repulsion or steric hindrance, depending on the type of

stabilizers employed. Its efficiency in increasing the reactivity of nZVI depends on the method of coating. For example, during post-synthesis stabilization with CMC, polyelectrolytes are physisorbed onto the particles surface, decreasing reactivity by blocking reactive surface sites and inhibiting diffusion of chlorinated compounds to the nanoparticles surface (Phenrat et al., 2009). On the other hand, during pre-synthesis stabilization with CMC, polyelectrolytes molecules are absorbed to the particle surface, resulting in a layer of negative charges and preventing agglomeration through electrostatic interactions that result in improved TCE dechlorination rates (He and Zhao, 2007).

2.2.3. Reactivity with Chlorinated Compounds

Nanoscale Zero Valent Iron (nZVI) particles are capable of degrading a wide range of chlorinated ethanes and ethenes. The ZVI (Fe^0) serves as the source of electrons and the chlorinated hydrocarbons as the electron acceptors (Li et al., 2006) with the rate of dechlorination increasing with the degree of chlorination (Gillham and Ohannesin, 1994). For example, Equation 2.9 shows the reduction of tetrachloroethene (PCE):

$$C_2Cl_4 + 4Fe^0 + 4H^+ \rightarrow C_2H_4 + 4Fe^{2+} + 4Cl^- \qquad \text{Eq. 2.9}$$

Dechlorination by ZVI involves the following steps (Matheson and Tratnyek, 1994): (1) Mass transport of the reactant to the Fe^0 surface from the bulk solution, (2) Adsorption of the reactant to the surface, (3) Chemical reaction at the surface, (4) Desorption of the products and (4) Mass transport of the products to the bulk solution.

nZVI reactions with chlorinated ethanes are slower than chlorinated ethenes and typically form chlorinated byproducts (Lien and Zhang, 2005). This is of great concern for field application since some of the byproducts formed might be more toxic that the parent compound. For

example, reductive dechlorination (breaking of carbon-chloride bonds via electron transfer reactions) of 1,1,2-trichloroethane to vinyl chloride. To avoid the formation of chlorinated byproducts and achieve complete dechlorination to ethane, bimetallic nanoparticles have been employed. For example, when monometallic nanoiron was used to degrade chlorinated ethanes, the major products mostly involved chlorinated ethenes (Song and Carraway, 2005). On the other hand, when bimetallic nano iron was used (Fe/Pd), complete dechlorination to ethane was observed (Lien and Zhang, 2005).

2.3. 1,2-Dichloroethane

1,2-Dichloroethane is a volatile organic compound used primarily for the production of vinyl chloride monomer (VCM), which is used in the production of polyvinyl chloride (PVC) plastic. It is also used in the manufacture of trichloroethane, trichloroethylene, paint, varnish and finish removers, soaps and scouring compounds and as a component of metal-degreasing formulations (IARC, 1999). 1,2-DCA has not been produced in Canada since 2006, but in 1990 its total annual production was estimated to be 992 thousand tonnes (IARC, 1999). Currently, 1,2-DCA is classified as a probable human carcinogen by the International Agency for Research on Cancer (IARC) (Group 2B) and by the U.S. EPA (Group B2) (Health-Canada, 2012). 1,2-DCA is readily absorbed by humans and has shown to adversely affect the immune system, liver, kidneys, lungs and cardiovascular system. In Canada, an interim maximum acceptable concentration for 1,2-DCA in drinking water of 5 μg/L has been established, though a maximum acceptable concentration of the same value was proposed in 2012 (Health-Canada, 2012).

2.3.1. Reactivity

1,2-Dichloroethane remains unreactive towards monometallic and bimetallic (Pd/Fe) iron nanoparticles (Lien and Zhang, 2001, Lien and Zhang, 2005, Song and Carraway, 2005). Song and Carraway (2005) reported that all chlorinated ethanes, except 1,2-DCA, were transformed to less chlorinated ethanes or ethenes. Lien and Zhang (2005) evaluated the potential of bimetallic nanoparticles (Pd/Fe) to dechlorinate 1,2-DCA but less than 5% degradation was observed within 24 hours of reaction. Other zero valent metals, such as Zn^0, have been used to degrade 1,2-DCA, but only with marginal success (Arnold et al., 1999, Vanstone et al., 2008). Zero valent zinc is a more powerful reductant than iron with a standard reduction potential of -0.76 V, however, even when very high concentrations of zinc were used (600 g/L), only 30 – 40 % degradation was achieved over 12 days (Vanstone et al., 2008). The extreme reductive recalcitrance of 1,2-DCA has been attributed to the low oxidation state of the carbon atoms carrying the chlorine atoms (-1) (De Wildeman and Verstraete, 2003). But recent studies have suggested that under very strong reducing conditions (ORP of at least -1100 mV), degradation of 1,2-DCA is possible (Huang et al., 2011, Liu et al., 2014, Yoon et al., 2014). Huang et al. (2011) studied the dechlorination of 1,2-DCA using copper nanoparticles as a surface and hydrogenation catalyst and sodium borohydride as an electron donor. 85% degradation was achieved within 5 hours with ethane accounting for 79% and ethene for 1.1% of the products. It was found that 1,2-DCA could not be reduced in the presence of copper nanoparticles alone or under borohydride reduction alone, meaning that the reaction is surface mediated and occurs only under strong reducing conditions. Successful degradation of 1,2-DCA has also been achieved using advanced reduction processes (ARPs), which consist of the combination of

ultraviolet (UV) light irradiation and a reductant to produce highly reactive species (Equations 2.10 - 2.11) (Liu et al., 2014, Yoon et al., 2014).

Sulfite/UV ARP $SO_3^{2-} + h\nu \rightarrow SO_3^{*-} + e_{aq}^-$ Eq. 2.10

Dithionite/UV ARP $S_2O_4^{2-} + h\nu \rightarrow 2SO_2^{*-}$ Eq. 2.11

In the ARP method, degradation is due to the reaction of 1,2-DCA and the reactive species produced after the reducing agent is activated with the ultra-violet light. For example, in the sulfite/UV ARP system, the major species responsible for the reduction of 1,2-DCA was the aqueous electron (Liu et al., 2014). This corroborates the importance of creating strong reducing conditions for the dechlorination of 1,2-DCA. Table 2.1 shows a summary of the studies mentioned above.

Table 2.1 Zero Valent Metals/Reductants for 1,2-DCA Degradation

Author	Treatment	Degradation	Products	Pathways	Notes
Arnold et al., 1999	**Metal:** Zn^0 (30 mesh size) Conc.: 60.6 g/L	Not specified	Ethylene	β-elimination	Conversion was insufficient for the calculation of rate constant
Lien and Zhang., 2005	**Metal:** Pd/Fe Nanoparticles Conc.: 5 g/L	(< 5%)	N/A	N/A	No measurable (< 5%) reduction of 1,2-DCA was observed within 24 hours
Song and Carraway, 2005	**Metal:** nZVI Conc.: 0.625 g/L	None	N/A	N/A	DCA isomers monitored over 40 days 1,2-DCA showed no sign of transformation
Vanstone et al., 2008	**Metal:** Zn^0 (30 mesh size) Conc.: 600 g/L	30-40 % in 12 days	Ethene	β-elimination	After 12 days, excess H_2 gas generation hindered collection of samples
Huang et al., 2011	**Metal:** Cu^0 Nanoparticles Conc.: 2.5 g/L **Reductant:** NaBH4 = 25 mM	85 % within 5 hours	Ethane: 79 % Ethylene: 1.1 %	Hydrogenolysis Dihaloelimination	Degradation rate is a function of the reducing power
Liu et al., 2013	UV Light + Sulfite	100%	Not specified	Not specified	Aqueous electron responsible for degradation
Yoon et al., 2013	UV Light + Dithionite	100%	Not specified	Not specified	Degradation attributed to sulfur dioxide radicals

Even though the use of copper nanoparticles with a reductant has been found to achieve greater than 80% degradation of 1,2-DCA, the use of copper nanoparticles is undesirable because of potential contamination caused by copper ions (Huang et al., 2011). Since the reaction only occurred in the presence of a surface under strong reducing conditions, a formulation using nZVI with a strong reductant, other than sodium borohydride, is an attractive alternative.

2.4. Sodium Dithionite

One of the most common reductants used in the remediation field is sodium dithionite (reduction potential of -1.12 V). This reducing agent is used in the creation of Permeable Reactive Barriers (PRB) in a technique called In-Situ Redox Manipulation (ISRM). In this technique, a reductant is added to the subsurface to reduce naturally occurring ferric iron (Fe(III)) to ferrous iron (Fe(II)) (Equation 2.12). This in turn will serve as an electron donor for the reduction of redox-sensitive contaminants (e.g., chromate, chlorinated solvents) flowing through the reduced zone (Equation 2.13) (Amonette et al., 1994).

$$S_2O_4^{2-}(aq) + 2Fe^{3+}(s) + 2H_2O \rightarrow 2SO_3^{2-}(aq) + 2Fe^{2+}(s) + 4H^+ \qquad \text{Eq. 2.12}$$

$$CrO_4^{2-}(aq) + 3\,Fe^{2+}(s) + 5H^+ \rightarrow Cr(OH)_3(s) + 3Fe^{3+} + H_2O \qquad \text{Eq. 2.13}$$

Among its industrial uses, sodium dithionite is widely employed in the reduction of vat dyes in the textile and paper industries (Makarov and Silaghi-Dumitrescu, 2013). The high reactivity of dithionite is due to its long and weak S-S bond (2.39 Å) which allows the dithionite ion ($S_2O_4^{2-}$) to reversibly dissociate into two sulphoxyl radicals (SO_2^{*-}) (Amonette et al., 1994). These free radicals are very strong reductants and are responsible for the reducing power of dithionite (Equation 2.14).

$$4SO_2^{*-} \leftrightarrow 2S_2O_4^{2-} \qquad \text{Eq. 2.14}$$

Sulphoxyl Radicals — Dithionite

In aqueous solution, dithionite is very unstable, undergoing a disproportionation reaction to yield sulfite (SO_3^-), thiosulfate ($S_2O_3^{2-}$) and hydrogen ions (Equation 2.15). This reaction is favored at acidic pH and at high concentrations. In the same way, at pH below 6, thiosulfate can undergo a disproportionation reaction yielding sulfate and hydrogen sulfide (Equation 2.16).

$$2S_2O_4^{2-} + H_2O \rightarrow 2SO_3^{2-} + S_2O_3^{2-} + 2H^+ \qquad \text{Eq. 2.15}$$

$$S_2O_3^{2-} + H_2O \rightarrow H_2S + SO_4^{2-} \qquad \text{Eq. 2.16}$$

On the other hand, at neutral and basic pH, sulfite and thiosulfate can also serve as reductants following their oxidation to sulfate (Equations 2.17 – 2.18).

$$2SO_3^{2-} + 2H_2O \leftrightarrow 2SO_4^{2-} + 4e^- + 4H^+ \qquad \text{Eq. 2.17}$$

$$S_2O_3^{2-} + 5H_2O \leftrightarrow 2SO_4^{2-} + 8e^- + 10H^+ \qquad \text{Eq. 2.18}$$

When compared to other reducing agents (e.g., thiosulfate, sulfide, hydrazine), dithionite was found to be the most effective chemical for the reduction of structural Fe in smectite (Gan et al., 1992). Besides being a strong reductant, dithionite and its reaction products are relatively nontoxic, making it the preferred reductant for ISRM (Nzengung et al., 2001).

2.4.1. nZVI and Sodium Dithionite

Research combining dithionite and nZVI has been conducted in recent years. Feitz et al. (2004) developed a method for synthesizing nZVI using dithionite ($nZVI_{S2O4}$) as a reductant instead of the well-known method using sodium borohydride ($nZVI_{BH4}$). This method consists of the reduction of a ferrous ion solution ($FeSO_4$ or $FeCl_2$) with sodium dithionite under alkaline conditions in an inert atmosphere (Equations 2.19 – 2.21) (Feitz et al., 2004). At a pH range between 9 and 11, Fe^{2+} will be reduced to Fe^0 according to the following reactions:

Half-reaction: $S_2O_4^{2-} + 4OH^- \rightarrow 2SO_3^{2-} + 2H_2O + 2e^-$ Eq. 2.19

Half-reaction: $Fe^{2+} + 2e^- \rightarrow Fe_{(s)}$ Eq. 2.20

Overall-reaction: $S_2O_4^{2-} + Fe^{2+} + 4OH^- \rightarrow Fe_{(s)} + 2SO_3^{2-} + 2H_2O$ Eq. 2.21

The particles formed with this method are very thin platelets, unlike the spherical particles obtained using the borohydride reduction method. Sun et al. (2008) compared the reactivity of $nZVI_{S2O4}$ and $nZVI_{BH4}$ towards trichloroethylene (TCE) degradation and found that $nZVI_{S2O4}$ nanoparticles have similar reactivity to that of $nZVI_{BH4}$. Dithionite has also been used in combination with sodium borohydride to synthesize Fe/FeS nanoparticles (Kim et al., 2011). In this approach, dithionite is mixed with the borohydride solution prior to its addition to the iron precursor. The goal of this method is to synthesize iron nanoparticles coated with iron sulfides (FeS). Iron sulfides are good semiconductors because of delocalized electrons in its layers. It is expected that its deposition on the nZVI outer layer will facilitate the conduction of electrons from the iron core to the adsorbed contaminants, resulting in higher reaction rates (Kim et al., 2011). Increased TCE dechlorination rates were observed as well as morphological changes, such as higher roughness of Fe/FeS nanoparticles, when compared to the pristine Fe (Kim et al., 2011). In this approach, however, dithionite is only used as a sulfide (S^{2-}) precursor for Fe/FeS synthesis and it is not directly involved in the reactivity. Dithionite has also been proposed as a suitable reductant to restore the reducing capacity of passivated nZVI (Xie and Cwiertny, 2010).

2.5. Summary

The higher reactivity and nano-scale size of nZVI helps overcome the limitations encountered using micro zero valent iron. To further increase its reactivity, nZVI is stabilized with polymers to avoid agglomeration and doped with noble metals to allow for the utilization of hydrogen gas

derived from the oxidation of iron with water. Though nZVI has proven to be effective for the degradation of chlorinated ethanes and ethenes, its reactivity towards 1,2-DCA has been negligible (<5 % degradation). It has been proposed that abiotic degradation of 1,2-DCA is possible but only under strong reducing conditions. To provide the reducing conditions necessary to degrade 1,2-DCA, a combination of sodium dithionite and nZVI is proposed in this research work.

2.6. References

Amonette, J. E., J. E. Szecsody, H. T. Schaef, Y. A. Gorby, J. S. Fruchter and J. C. Templeton (1994). Abiotic reduction of aquifer materials by dithionite: A promising in-situ remediation technology. Conference: 33. Hanford symposium on health and the environment: symposium on in-situ remediation--scientific basis for current and future technologies, Richland, WA (United States), 7-11 Nov 1994; Other Information: PBD: Nov 1994**:** Medium: ED; Size: 53 p.

Arnold, W. A., W. P. Ball and A. L. Roberts (1999). "Polychlorinated ethane reaction with zero-valent zinc: pathways and rate control." Journal of Contaminant Hydrology **40**(2): 183-200.

De Wildeman, S. and W. Verstraete (2003). "The quest for microbial reductive dechlorination of C-2 to C-4 chloroalkanes is warranted." Applied Microbiology and Biotechnology **61**(2): 94-102.

Feitz, A. J., J. Guan and T. D. Waite (2004). Process for Producing a Nanoscale Zero-Valent Metal. Australia, CRC For Waste Management and Pollution Control Limited.

Gan, H., J. W. Stucki and G. W. Bailey (1992). "Reduction of Structural Iron in Ferruginous Smectite by Free-Radicals." Clays and Clay Minerals **40**(6): 659-665.

Gillham, R. W. and S. F. Ohannesin (1994). "Enhanced Degradation of Halogenated Aliphatics by Zero-Valent Iron." Ground Water **32**(6): 958-967.

He, F. and D. Y. Zhao (2005). "Preparation and characterization of a new class of starch-stabilized bimetallic nanoparticles for degradation of chlorinated hydrocarbons in water." Environmental Science & Technology **39**(9): 3314-3320.

He, F. and D. Y. Zhao (2007). "Manipulating the size and dispersibility of zerovalent iron nanoparticles by use of carboxymethyl cellulose stabilizers." Environmental Science & Technology **41**(17): 6216-6221.

Health-Canada (2012). 1,2-Dichloroethane in Drinking Water. F.-P.-T. C. o. D. Water. Ottawa, Ontario.

Huang, C. C., S. L. Lo, S. M. Tsai and H. L. Lien (2011). "Catalytic hydrodechlorination of 1,2-dichloroethane using copper nanoparticles under reduction conditions of sodium borohydride." Journal of Environmental Monitoring **13**(9): 2406-2412.

IARC (1999). Monographs on the Evaluation of the Carcinogenic Risk of Chemicals to Humans. Re-evaluation of Some Organic Chemicals, Hydrozine and Hydrogen Peroxide (Part Two). Lyon, World Health Organization. **Vol. 71:** 501-529.

Kim, E. J., J. H. Kim, A. M. Azad and Y. S. Chang (2011). "Facile Synthesis and Characterization of Fe/FeS Nanoparticles for Environmental Applications." Acs Applied Materials & Interfaces **3**(5): 1457-1462.

Li, X.-q., D. W. Elliott and W.-x. Zhang (2006). "Zero-Valent Iron Nanoparticles for Abatement of Environmental Pollutants: Materials and Engineering Aspects." Critical Reviews in Solid State and Materials Sciences **31**(4): 111-122.

Lien, H. L. and W. X. Zhang (2001). "Nanoscale iron particles for complete reduction of chlorinated ethenes." Colloids and Surfaces a-Physicochemical and Engineering Aspects **191**(1-2): 97-105.

Lien, H. L. and W. X. Zhang (2005). "Hydrodechlorination of chlorinated ethanes by nanoscale Pd/Fe bimetallic particles." Journal of Environmental Engineering-Asce **131**(1): 4-10.

Liu, X., B. P. Vellanki, B. Batchelor and A. Abdel-Wahab (2014). "Degradation of 1,2-dichloroethane with advanced reduction processes (ARPs): Effects of process variables and mechanisms." Chemical Engineering Journal **237**(0): 300-307.

Liu, Y. Q., H. Choi, D. Dionysiou and G. V. Lowry (2005). "Trichloroethene hydrodechlorination in water by highly disordered monometallic nanoiron." Chemistry of Materials **17**(21): 5315-5322.

Makarov, S. V. and R. Silaghi-Dumitrescu (2013). "Sodium dithionite and its relatives: past and present." Journal of Sulfur Chemistry **34**(4): 444-449.

Matheson, L. J. and P. G. Tratnyek (1994). "Reductive Dehalogenation of Chlorinated Methanes by Iron Metal." Environmental Science & Technology **28**(12): 2045-2053.

Nzengung, V. A., R. M. Castillo, W. P. Gates and G. L. Mills (2001). "Abiotic transformation of perchloroethylene in homogeneous dithionite solution and in suspensions of dithionite-treated clay minerals." Environmental Science & Technology **35**(11): 2244-2251.

O'Carroll, D., B. Sleep, M. Krol, H. Boparai and C. Kocur (2013). "Nanoscale zero valent iron and bimetallic particles for contaminated site remediation." Advances in Water Resources **51**: 104-122.

Phenrat, T., Y. Q. Liu, R. D. Tilton and G. V. Lowry (2009). "Adsorbed Polyelectrolyte Coatings Decrease Fe-0 Nanoparticle Reactivity with TCE in Water: Conceptual Model and Mechanisms." Environmental Science & Technology **43**(5): 1507-1514.

Phenrat, T., N. Saleh, K. Sirk, R. D. Tilton and G. V. Lowry (2007). "Aggregation and sedimentation of aqueous nanoscale zerovalent iron dispersions." Environmental Science & Technology **41**(1): 284-290.

Saleh, N., K. Sirk, Y. Q. Liu, T. Phenrat, B. Dufour, K. Matyjaszewski, R. D. Tilton and G. V. Lowry (2007). "Surface modifications enhance nanoiron transport and NAPL targeting in saturated porous media." Environmental Engineering Science **24**(1): 45-57.

Schrick, B., B. W. Hydutsky, J. L. Blough and T. E. Mallouk (2004). "Delivery vehicles for zerovalent metal nanoparticles in soil and groundwater." Chemistry of Materials **16**(11): 2187-2193.

Song, H. and E. R. Carraway (2005). "Reduction of chlorinated ethanes by nanosized zero-valent iron: Kinetics, pathways, and effects of reaction conditions." Environmental Science & Technology **39**(16): 6237-6245.

Sun, Q., A. J. Feitz, J. Guan and T. D. Waite (2008). "COMPARISON OF THE REACTIVITY OF NANOSIZED ZERO-VALENT IRON (nZVI) PARTICLES PRODUCED BY BOROHYDRIDE AND DITHIONITE REDUCTION OF IRON SALTS." Nano **3**(5): 341-349.

Sun, Y. P., X. Q. Li, J. Cao, W. X. Zhang and H. P. Wang (2006). "Characterization of zero-valent iron nanoparticles." Adv Colloid Interface Sci **120**(1-3): 47-56.

Tiraferri, A., K. L. Chen, R. Sethi and M. Elimelech (2008). "Reduced aggregation and sedimentation of zero-valent iron nanoparticles in the presence of guar gum." Journal of Colloid and Interface Science **324**(1-2): 71-79.

Vanstone, N., M. Elsner, G. Lacrampe-Couloume, S. Mabury and B. S. Lollar (2008). "Potential for identifyng abiotic chloroalkane degradation mechanisms using carbon isotopic fractionation." Environmental Science & Technology **42**(1): 126-132.

Wang, C. B. and W. X. Zhang (1997). "Synthesizing nanoscale iron particles for rapid and complete dechlorination of TCE and PCBs." Environmental Science & Technology **31**(7): 2154-2156.

Xie, Y. and D. M. Cwiertny (2010). "Use of Dithionite to Extend the Reactive Lifetime of Nanoscale Zero-Valent Iron Treatment Systems." Environmental Science & Technology **44**(22): 8649-8655.

Yan, W., H.-L. Lien, B. E. Koel and W.-x. Zhang (2013). "Iron nanoparticles for environmental clean-up: recent developments and future outlook." Environmental Science: Processes & Impacts **15**(1): 63.

Yoon, S., D. S. Han, X. Liu, B. Batchelor and A. Abdel-Wahab (2014). "Degradation of 1,2-dichloroethane using advanced reduction processes." Journal of Environmental Chemical Engineering **2**(1): 731-737.

Zhang, W.-x. and D. W. Elliott (2006). "Applications of iron nanoparticles for groundwater remediation." Remediation Journal **16**(2): 7-21.

Chapter 3

3. Enhanced dechlorination of 1,2-dichloroethane by coupled nano iron - dithionite treatment.

3.1. Introduction

Chlorinated solvents are amongst the most frequently detected organic contaminants in groundwater due to their extensive production, industrial application and improper handling and disposal (Stroo et al., 2003, Moran et al., 2006, O'Carroll et al., 2013). 1,2-dichloroethane (1,2-DCA) is a chlorinated solvent used predominantly in the manufacture of the vinyl chloride monomer and is one of the most commonly found substances at US EPA Superfund Sites (ATSDR, 2001, U.S.EPA, 2014). It is classified as a probable human carcinogen and causes neurological disorders as well as liver and kidney diseases (IARC, 1999, ATSDR, 2001, Health-Canada, 2012).

Biodegradation of 1,2-DCA is possible under aerobic and anaerobic conditions using microbial isolates (Maymo-Gatell et al., 1999, De Wildeman et al., 2004, Smidt and de Vos, 2004, Le and Coleman, 2011). However, in the presence of other halogenated compounds, 1,2-DCA dechlorination by microbial communities is severely inhibited (Yu et al., 2013). Since chlorinated solvents are frequently found in mixtures at contaminated sites (Moran et al., 2006), this limits the bioremediation of 1,2-DCA.

Abiotic degradation of 1,2-DCA in the aqueous phase has been reported under strong reducing conditions using advanced reduction processes (ARP), and copper nanoparticles coupled with sodium borohydride (Huang et al., 2011, Liu et al., 2014, Yoon et al., 2014). For the ARP system, ultraviolet light (UV) irradiation was used to activate reducing agents (e.g., sulfite, dithionite, sulfide) to degrade 1,2-DCA. Complete dechlorination of 1,2-DCA was attributed to

its reaction with highly reactive species (i.e., sulfoxyl radical, sulfite radical, aqueous electron, hydrogen atom, and excited state bisulfide ion) (Liu et al., 2014, Yoon et al., 2014). Approximately 85% degradation of 1,2-DCA to ethane was achieved using copper nanoparticles (Cu^0) in the presence of sodium borohydride (Huang et al., 2011). Copper is not a strong reductant (Eh = +0.38 V) and was used mainly as a hydrogenation catalyst for hydrodechlorination. Therefore, this treatment depends on the reducing capacity of sodium borohydride. The authors concluded that successful degradation of 1,2-DCA with copper nanoparticles requires an ORP lower than -1100 mV (Eh = -900 mV). One concern with this approach is subsurface copper contamination due to application of copper nanoparticles (Huang et al., 2011).

Reductive dechlorination of 1,2-DCA by zero valent metals, such as nano-scale zero valent iron (Fe^0, Eh = -0.44 V) and zero-valent zinc (Zn^0, Eh = -0.77 V), have had limited success (Arnold et al., 1999, Song and Carraway, 2005, Vanstone et al., 2008). Even when treated with concentrations of up to 600 g/L of Zn^0, only 30 to 40% 1,2-DCA degradation was observed (Vanstone et al., 2008).

Nano-scale zero valent iron (nZVI) has been extensively studied due its high reactivity with chlorinated hydrocarbons, chlorinated pesticides, nitro aromatic compounds, polychlorinated biphenyls (PCBs) and metals (O'Carroll et al., 2013). In aqueous solutions, nZVI reacts with water and dissolved oxygen to form ferrous iron and hydrogen gas (Equations 3.1 – 3.2).

$$Fe^0 + 2H_2O \rightarrow Fe^{2+} + H_2 + 2OH^- \qquad \text{Eq. 3.1}$$

$$2Fe^0 + O_2 + 2H_2O \rightarrow 2Fe^{2+} + 4OH^- \qquad \text{Eq. 3.2}$$

Ferrous iron can be further oxidized to ferric iron and react with hydroxides and water forming iron oxides and iron (oxy)hydroxides, such as magnetite (Fe_3O_4) and lepidocrocide (FeOOH) (Nurmi et al., 2005, Filip et al., 2014). Magnetite is one of the main oxidized forms of iron formed on the surface of nZVI, but it is not considered a strong reductant for reductive dechlorination of organic compounds (Lee and Batchelor, 2002) Thus far, nZVI has been unable to dechlorinate 1,2-DCA (Lien and Zhang, 2005, Song and Carraway, 2005). Out of the eight chlorinated ethanes treated with nZVI by Song and Carraway (2005), only 1,2-DCA was not transformed to less chlorinated compounds. nZVI is often doped with palladium to increase its reactivity, a combination referred to as bimetallic nZVI (O'Carroll et al., 2013). However, even use of bimetallic nZVI (Pd/Fe) yielded <5% 1,2-DCA degradation in 24 hours (Lien and Zhang, 2005).

As such nZVI alone does not provide the strong reducing conditions suggested by Huang et al. (2011) necessary to dechlorinate 1,2-DCA. Even coupling nZVI with borohydride could not dechlorinate dichloromethane (DCM, another recalcitrant chlorinated hydrocarbon) which otherwise was completely dechlorinated by the combination of nano Cu^0-borohydride (Huang et al., 2012). This indicates that the effectiveness of sodium borohydride for reductive dechlorination of chlorinated compounds is dependent on the catalytic properties of the metal used in the system. The use of iron as a hydrogenation catalyst usually requires high temperatures (~ 495 K) and pressures (>15 bar) (Pyatnitskii et al., 1996, Daida and Peters, 2004, Liu et al., 2005). The activation of hydrogen by iron nanoparticles is highly dependent on its morphology, with poorly ordered nanoparticles (amorphous) being more effective than its well crystalline analogue (Liu et al., 2005). The limitations of nZVI as hydrogenation catalysts make it unsuitable to activate the high quantities of hydrogen generated through the hydrolysis of

sodium borohydride (Muir and Yao, 2011). Therefore, an alternative treatment involving nZVI and a secondary reductant, other than sodium borohydride, is proposed in this work.

Sodium dithionite, a strong reductant (Eh = -1.12 V), has been successfully used as an In-Situ Redox Manipulation (ISRM) technology for treating various organic and inorganic contaminants (Fruchter et al., 2000, Szecsody et al., 2004, Boparai et al., 2006, Boparai et al., 2008). ISRM involves injection of dithionite to the subsurface to reduce ferric iron (Fe^{3+}) in soil/sediments to ferrous iron (Fe^{2+}) and creating an in-situ permeable reactive barrier for the reduction of contaminants migrating through the reduced zone (e.g., chromate, TCE) (Equation 3.3) (Amonette et al., 1994, Fruchter et al., 1994, Fruchter et al., 2000):

$$S_2O_4^{2-}(aq) + 2Fe^{3+}(s) + 2H_2O \rightarrow 2SO_3^{2-}(aq) + 2Fe^{2+}(s) + 4H^+ \qquad \text{Eq. 3.3}$$

Dithionite dissociates to two sulphoxyl radicals and, in aqueous solutions, reacts with water to yield sulfite and thiosulfate (Equations 3.4 - 3.5), which in turn can also serve as reductants under neutral and basic conditions.

$$4SO_2^{*-} \leftrightarrow 2S_2O_4^{2-} \qquad \text{Eq. 3.4}$$

$$2S_2O_4^{2-} + H_2O \rightarrow 2SO_3^{2-} + S_2O_3^{2-} + 2H^+ \qquad \text{Eq. 3.5}$$

Decomposition products of dithionite further react with Fe^{2+} to form iron sulfides (FeS) and polysulfides (Fe_xS_y) (Nzengung et al., 2001, Langell et al., 2009) which are capable of dechlorinating select chlorinated hydrocarbons but not 1,2-DCA (Kriegman-King and Reinhard, 1994, Butler and Hayes, 2000). Aqueous solutions of dithionite are also capable of reducing chlorinated hydrocarbons via reductive dechlorination and nucleophilic substitution (Rodriguez and Rivera, 1997, Nzengung et al., 2001). Dithionite and its reaction products are considered relatively nontoxic and thus offer an environmentally suitable means of treating contaminated

groundwater (Nzengung et al., 2001). Moreover, the ISRM treatment zones are reported to remain anoxic for several years increasing the longevity of this technology (Fruchter et al., 2000). The overall success of ISRM, however, depends upon the availability of sufficient dithionite-reducible iron associated with the soil/sediments in the subsurface. Thus, coupling the nZVI and ISRM (dithionite) is expected to make this remediation technology more effective.

Dithionite has also been used to extend the reactive lifespan of oxidized nZVI (Xie and Cwiertny, 2010), and for synthesizing Fe/FeS or Fe^0 nanoparticles with or without sodium borohydride (Feitz et al., 2004, Kim et al., 2011). Particles synthesized in these studies were thoroughly washed to remove any excess dithionite and its decomposition products in the supernatant. As such, the long-term influence of aqueous dithionite and its decomposition products on nZVI reactivity has not been investigated.

The objectives of this research are to : (a) develop an nZVI/dithionite formulation capable of dechlorinating 1,2-DCA; (b) assess the effect of dithionite on the reactivity and longevity of nZVI and (c) study the morphology and surface properties of nZVI pre- and post-dithionite addition

3.2. Materials and Methods

3.2.1. Chemicals

All chemicals were used as received: $FeSO_4.7H_2O$ (99.5% ACROS Organics), K_2PdCl_6 (99%, Alfa Aesar, Pd min 26.69%), Sodium Carboxymethyl Cellulose (90K , ACROS Organics), NaCl (EMD Chemicals Inc), $NaBH_4$ (98+%, ACROS Organics), $Na_2S_2O_4$ (88% , J.T. Baker), $Na_2S_2O_4$ (85% , Sigma-Aldrich), 1,1,2-Trichloroethane (1,1,2-TCA) (98%, ACROS Organics), Trichloethene (TCE) (99.5%, Alfa Aesar), 1,2-Dichloroethane (1,2-DCA) (99+%, Sigma-

Aldrich), $FeCl_2.4H_2O$ (98%, Alfa Aesar), $FeCl_3.6H_2O$ (97%, Alfa Aesar), $Na_2S.9H_2O$ (99.99+ %, Sigma-Aldrich), Gas Mix (5% H_2 balance Ar, PRAXAIR), N_2 (Ultra High Purity, PRAXAIR).

3.2.2. Experimental System

nZVI, magnetite and iron sulfide synthesis was performed inside an anaerobic glove box (Coy Laboratory Products, Inc) under a 95% Ar : 5% H_2 atmosphere. All experiments were conducted with deionized (DI) water, purged for two hours with ultra-high purity nitrogen to remove dissolved oxygen. For the bare-nZVI, a solution of $FeSO_4.7H_2O$ was titrated with a $NaBH_4$ solution to reduce ferrous iron to zero-valent iron (Equation 3.6) (Zhang and Elliott, 2006):

$$2Fe^{2+} + BH_4^- + 3H_2O \rightarrow 2Fe^0 + H_2BO_3^- + 4H^+ + 2H_2 \qquad \text{Eq. 3.6}$$

The mixture turned black after the addition of $NaBH_4$, the characteristic color of Fe^0 nanoparticles. The solution was mixed for 20 min to ensure complete reduction of the iron precursor. The nanoparticles were washed thrice with deoxygenated DI water after stirring and a palladium loading of 0.5% w/w of iron was added (Equation 3.7) using K_2PdCl_6 dissolved in 3.42 mM NaCl.

$$PdCl_6^{2-} + 2Fe^0 \rightarrow Pd^0 + 2Fe^{2+} + 6Cl^- \qquad \text{Eq. 3.7}$$

Stabilized nanoparticles were synthesized using the pre-synthesis method with carboxymethyl cellulose (CMC 90K) (Sakulchaicharoen et al., 2010). The CMC solution was dissolved overnight and deoxygenated for two hours using ultra-high purity nitrogen. The Fe^{2+} precursor was mixed with CMC for 5 min before the drop-wise addition of $NaBH_4$. The final mixture was stirred for 30 min and then spiked with a 0.5% w/w solution of K_2PdCl_6. A 66 mM or 132 mM sodium dithionite ($Na_2S_2O_4$) stock solution was prepared inside the anaerobic golvebox with de-

oxygenated water and the desired amount was immediately added to the nZVI slurry in the reactor bottles.

Magnetite nanoparticles were prepared by co-precipitating $FeCl_3.6H_2O$ and $FeCl_2.4H_2O$ under alkaline conditions using NaOH (Equation 3.8) (Lopez et al., 2010):

$$2Fe^{3+} + Fe^{2+} + 4OH^- \rightarrow Fe_3O_4 + 4H^+ \qquad \text{Eq. 3.8}$$

After mixing 2.2 mL of 2M $FeCl_2.4H_2O$ with 8.6 mL of 1M $FeCl_3.6H_2O$, the reactants were magnetically stirred and set at an initial temperature of 30 ^oC. 1M NaOH was added drop-wise to maintain a pH of 12. The temperature was increased to 70 ^oC for 2 hours and then the system was cooled to room temperature. The precipitates were separated using a permanent magnet and washed 2 to 3 times with distilled, deoxygenated water. The final product was dried in a desiccator inside the anaerobic glovebox, maintaining anaerobic conditions at all times. The synthesis method for iron sulfide was adapted from Butler and Hayes (1998).

Reactivity experiments were conducted in 120 ml reactor bottles. For the experiments including nZVI, magnetite and iron sulfides, 60 ml of the synthesized nanoparticle was mixed with 30 ml of the sodium dithionite for a final 90 ml aqueous solution. Bottles were sealed inside the glove box with Mininert Valves. The reactors were immediately spiked with appropriate volumes of VOC stock solution (prepared in iso-propanol), using a gas-tight syringe. Table 3.1 summarizes VOC concentrations and treatment details of each reactivity experiment. The reactor bottles were shaken using either a wrist action shaker (Model 75, Burrell Inc.) or an orbital shaker at room temperature. Unless otherwise specified, two replicates were run for all experiments and with blanks consisting only of DI water and VOCs.

Table 3.1 Experimental Conditions of Reactivity Experiments

Exp. #	Dithionite (mM)	Metal (g/L)	CMC (w/v %)	Pd (w/w %)	VOC (µM)	*Kobs* (day^{-1})	Degradation (%)	Time (days)
1[*†]	44	nZVI = 5	1 %	0.5 %	1,2-DCA = 106	4.4×10^{-3}	79	386
2[*‡]	0, 22, 22	nZVI = 5	1 %	0.5 %	1,2-DCA = 106	3.8×10^{-3}	72	386
3[§]	22	nZVI = 5	1 %	0.5 %	1,2-DCA = 109	4.3×10^{-3}	76	397
4	22	nZVI =5	N/A	0.5 %	1,2-DCA = 123	7.8×10^{-3}	92	334
5	22	N/A	N/A	N/A	1,2-DCA = 142	2.1×10^{-3}	40	265
6	22	nZVI = 5	1 %	N/A	1,2-DCA = 156	4.5×10^{-3}	73	265
7	22	Fe_3O_4 = 5	N/A	N/A	1,2-DCA = 149	6.2×10^{-3}[‖]	50[‖]	116
8	22	nZVI = 2.5	1 %	N/A	1,2-DCA = 156	5.3×10^{-3}[‖]	45[‖]	112
9[¶†]	0	FeS = 5	N/A	N/A	1,2-DCA = 151	4.0×10^{-4}[‖]	4[‖]	116
10[¶]	22	FeS = 5	N/A	N/A	1,2-DCA = 149	4.7×10^{-3}[‖]	42[‖]	116
11	N/A	nZVI = 5	1 %	0.5 %	1,1,2-TCA = 855	3.3×10^{-1}	100	14
12	22	nZVI = 5	1 %	0.5 %	1,1,2-TCA = 897	7.3×10^{-3}	82	248
13	22	nZVI = 5	1 %	N/A	1,1,2-TCA = 876	9.7×10^{-3}	84	222

[*]Only one blank in a 1.5 % w/w CMC solution

[†]No reps

[‡]22 mM dithionite added twice, at 58 and 84 days

[§]Experiment spiked with 77 µM TCE at 140 days

[‖]% Degradation and k*obs* values calculated by subtracting the decrease of concentration observed in controls. See Appendix A for more information

3.2.3. Analytical Methods

Concentrations of 1,2-DCA, TCE and 1,1,2-TCA were analyzed with an Agilent 7890 Gas Chromatograph (GC) equipped with a DB-624 capillary column (75 m x 0.45 mm x 2.55 µm) and an Electron Capture Detector (ECD). The conditions of the GC method were as follows: N_2 as the carrier gas at a flow rate of 10 ml/min; a temperature ramp of 35 °C for 12 min, then 5 °C/min to 60 °C for 1 min and 17 °C/min to 200 °C for 5 min. These conditions were adapted from the EPA method 8021, used to determine volatile organic compounds.

Sampling was performed using the solvent extraction method with n-Hexane as the extracting solvent. 250 µL aqueous aliquot was collected from each reactor at a selected sampling time and mixed with 1 mL n-Hexane in a 2 mL GC vial. The GC vial was vortex-mixed and allowed to equilibrate for two hours before extraction. 1 µL of the extract was injected in split less mode by the GC auto sampler. Lower chlorinated products from the 1,1,2-TCA reactivity treatment were measured with an Agilent 7890A GC using a GS-GasPro Column (30 m x 320 µm I.D.) and a Flame Ionization Detector (FID). 250 µL aliquot was collected from each reactor and no extracting solvent used. The method parameters were as follows: He as the carrier gas at a flow rate of 2 ml/min with a temperature ramp of 35 °C for 5 min, then 10 °C/min to 220 °C for 7 min. A 250 µL headspace sample was withdrawn by the auto sampler and analyzed for possible dechlorination products, mainly ethane, ethylene and vinyl chloride (VC).

Characterization of the surface morphology of the iron nanoparticles was done using a scanning electron microscope (SEM, Hitachi S-4500 N, 10 kV). The solid samples were sprinkled onto adhesive carbon tape supported on metallic disk. The elemental composition of nZVI particles was determined by randomly selecting areas on the solid surfaces and analyzing by energy-

dispersive X-ray (EDX) in conjunction with SEM. Elemental composition and chemical state of the atoms present on the nZVI surface was performed with a Kratos Axis Ultra spectrometer (XPS), using a monochromatic Al Kα source (15 mZ, 14 kV). The instrument work function was calibrated to give a binding energy (BE) of 83.96 eV for the Au $4f_{7/2}$ line of metallic gold and the spectrometer dispersion was adjusted to give a BE of 932.62 eV for the Cu $2p_{3/2}$ line of metallic copper. The Kratos charge neutralizer system was used on all specimens. Survey scan analyses were carried out with an analysis area of 300 x 700 microns and pass energy of 160 eV. High resolution analyses were carried out with an analysis area of 300 x 700 microns and pass energy of 20 eV. Spectra have been charge corrected to the main line of the C 1s spectrum (adventitious carbon) set to 284.8 eV. Spectra were analyzed using CasaXPS software (version 2.3.14) (Fairley, 1999). Samples were mounted on a non-conductive adhesive tape and introduced into the vacuum via an attached argon filled glove box to prevent oxidation. The nanoparticle structure was investigated with a Rigaku RPT 300 RC diffractometer (Co Kα radiation, step size 0.02°, 2θ rage 10-70°).

The zerovalent iron content of the nZVI particles was measured using a gas volumetric based method (Equation 3.9) (de Boer, 2012).

$$Fe^0 + 2H^+ \rightarrow Fe^{2+} + H_2 \qquad \text{Eq. 3.9}$$

10 ml of 32 % (10 M) HCl was added to 0.1 g of iron. The volume of hydrogen (H_2) produced was calculated by measuring the water displaced following Eq. 3.9. The moles of H_2 were calculated from the volume of H_2 using the ideal gas law. The number of moles of H_2 produced is equal to the number of moles of Fe^0 present in the sample (Eq. 3.9).

3.3. Results and Discussion

3.3.1. Effect of Dithionite

Dithionite is expected to enhance reactivity of zero valent iron by providing electrons following its dissociation and disproportionation (Equations 3.4 – 3.5). To test the effect of dithionite on the reactivity of iron, a treatment with 5 g L^{-1} CMC-nZVI and 0.5% w/w Pd was evaluated with and without 44 mM dithionite (Exp. 1 and 2, respectively). Figure 3.1 shows the first 50 days of Exp. 1 and 2 to show the effect of dithionite at the early stage of the reactivity experiments.

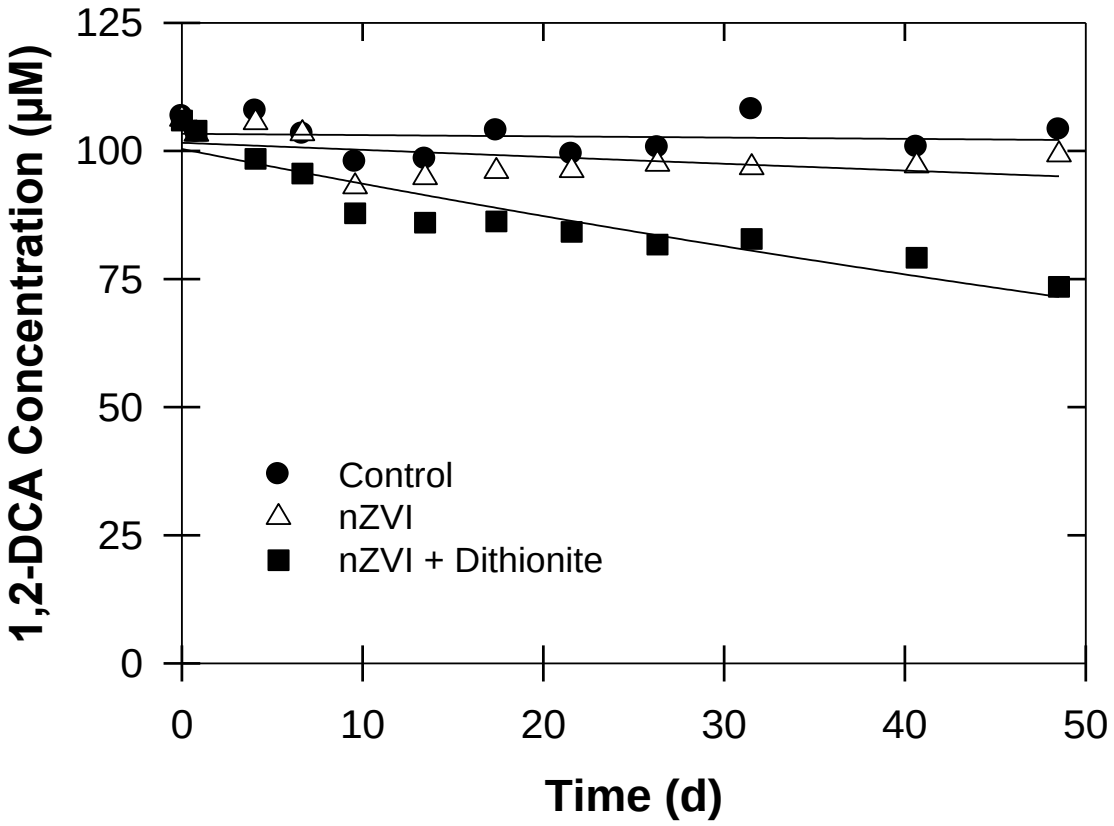

Figure 3.1 Effect of dithionite (44 mM) on 1,2-DCA degradation by 5.0 g L^{-1} CMC-nZVI + 0.5% w/w Pd. Square (nZVI + Dithionite) and circular (control) symbols represent results from a single reactor. Triangular symbols represent average concentrations from duplicate

reactors. Error bars are smaller than the symbols. Lines are pseudo-first order fittings of data points.

In the absence of dithionite (Exp. 2), only 9% degradation was achieved at the end of 13 days. After 13 days no further degradation was observed and at the end of 48 days, the nZVI suspension was completely oxidized and turned white forming ferrous hydroxide ($Fe(OH)_2$) (Leussing and Kolthoff, 1953). On the other hand, the treatment with 44 mM dithionite (Exp.1) achieved 28% degradation after 48 days with the solution maintaining its black color. These results suggest that dithionite coupled with nZVI enhances 1,2-DCA dechlorination. Magnetite (Exp. 7) and iron sulfide (Exp. 10) nanoparticles were also tested in the presence of 22 mM dithionite (Figure A1). Iron sulfides were unable to dechlorinate 1,2-DCA (Butler and Hayes, 2000) To show the effect of dithionite, an experiment with iron sulfides alone (i.e., no dithionite, Exp. 9) was performed. Magnetite is considered a very poor reductant for reductive dechlorination of organic compounds (Lee and Batchelor, 2002). As such, no separate experiment using only magnetite was conducted. As shown in Figure A1 and Table 3.1, the reaction rates of magnetite and iron sulfide coupled with dithionite are comparable to that of the nZVI-dithionite system. These nanoparticles would otherwise be unreactive towards 1,2-DCA, as is the case of the iron sulfides in Exp. 9 (Figure A1).

To test the ability of dithionite to restore the reducing capacity of oxidized nZVI, 44 mM dithionite was injected in two increments at 58 and 84 days to the oxidized iron from Exp. 2. After the first addition of dithionite, the oxidized iron solution turned black within 7 days and its reactivity with 1,2-DCA increased immediately, with a degradation rate similar to the experiment in which 44 mM dithionite was added initially (Figure 3.2). The effect of dithionite concentration

on 1,2-DCA degradation in the presence of nZVI was further studied by decreasing the dithionite concentration to 22 mM (Exp. 3). The experiment with 22 mM dithionite exhibited similar reactivity to that with 44 mM, indicating that a twofold concentration decrease has no impact on the reaction rate. Exp. 1 and 2 yielded 79% and 72% degradation of 106 μM 1,2-DCA, respectively, in 386 days. Similarly, Exp. 3 achieved 76% degradation of 109 μM 1,2-DCA in 397 days.

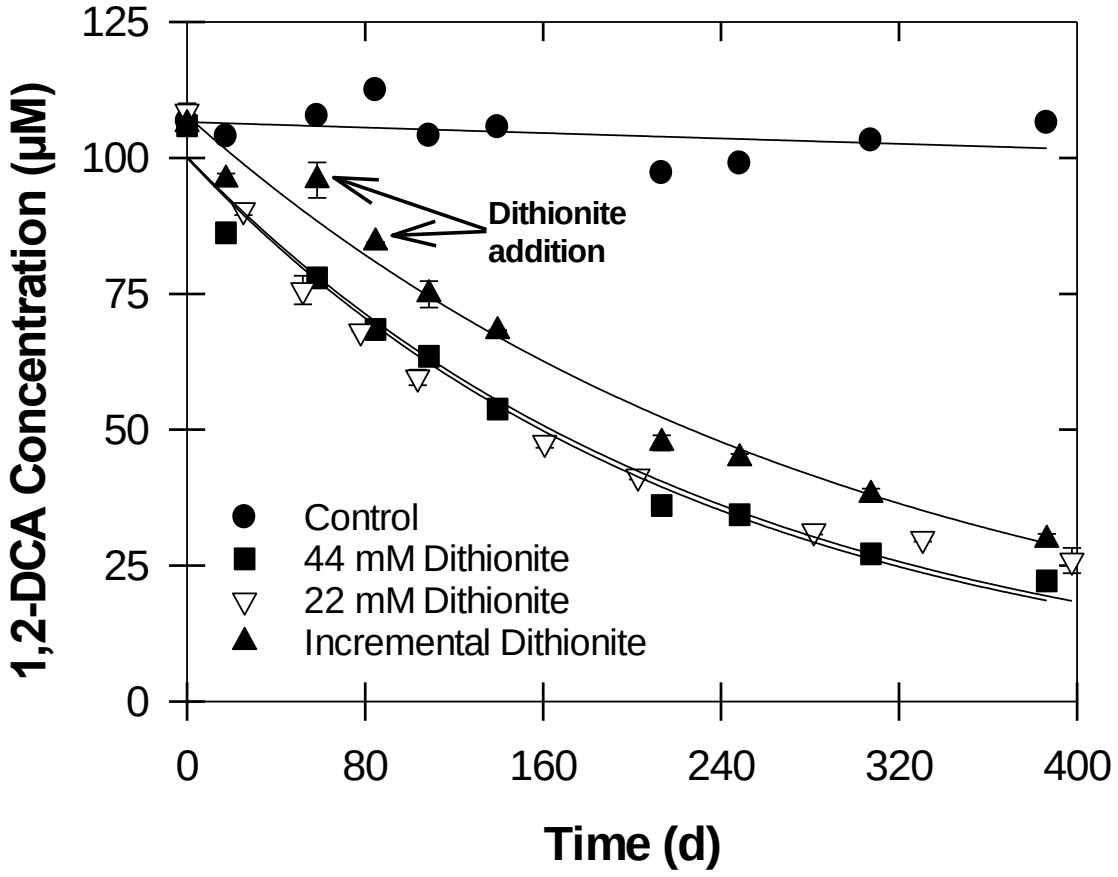

Figure 3.2 Effect of varying dithionite concentrations on 1,2-DCA degradation by 5 g L^{-1} CMC-nZVI + 0.5% w/w Pd. 22mM dithionite was added twice in the incremental dithionite treatment experiment at 58 and 84 days. Square (44 mM Dithionite) and circular (control) symbols represent results from a single reactor. Open (22 mM) and close (Incremental Dithionite) triangular symbols represent average concentrations from duplicate reactors.

Lines are pseudo-first order fittings of data points. In some cases, error bars are smaller than the symbols.

To confirm continued reactivity, the 22 mM dithionite-nZVI suspension (Exp. 3) was spiked with 77 μM TCE at 140 days. TCE was completely dechlorinated within 3 days following TCE addition (Figure A2), suggesting that the nZVI suspension was still reactive. The longevity of these experiments has far exceeded the typical reactive lifetime of CMC nZVI-Pd systems, which ranges between 6 to 12 days (He et al., 2010a).

3.3.2. Effect of nZVI

Dithionite is capable of degrading select chlorinated compounds and pesticides (Castillo et al., 1997, Rodriguez and Rivera, 1997, Nzengung et al., 2001, Liu et al., 2012). However, when combined with a reactive surface (e.g., alumina or iron) the reaction rate of the system increases (Nzengung et al., 2001, Liu et al., 2012). Therefore, a heterogeneous solution with nZVI is expected to show a higher reaction rate than a homogeneous solution of only dithionite. nZVI promotes target contaminant adsorption on its surface, in doing so facilitating the transfer of electrons from the iron core and/or the bulk solution to 1,2-DCA.

The effect of nZVI was evaluated by simultaneously running experiments with dithionite alone (Exp. 5) and dithionite + nZVI (Exp. 6) (Figure 3.3). The concentration of nZVI was 5 g L^{-1} in 1 % w/v CMC, when nZVI was present, and 22 mM dithionite for both experiments. To evaluate the effect of nZVI dosage, an experiment with 2.5 g L^{-1} was conducted separately (Exp. 8) (Figure A1).

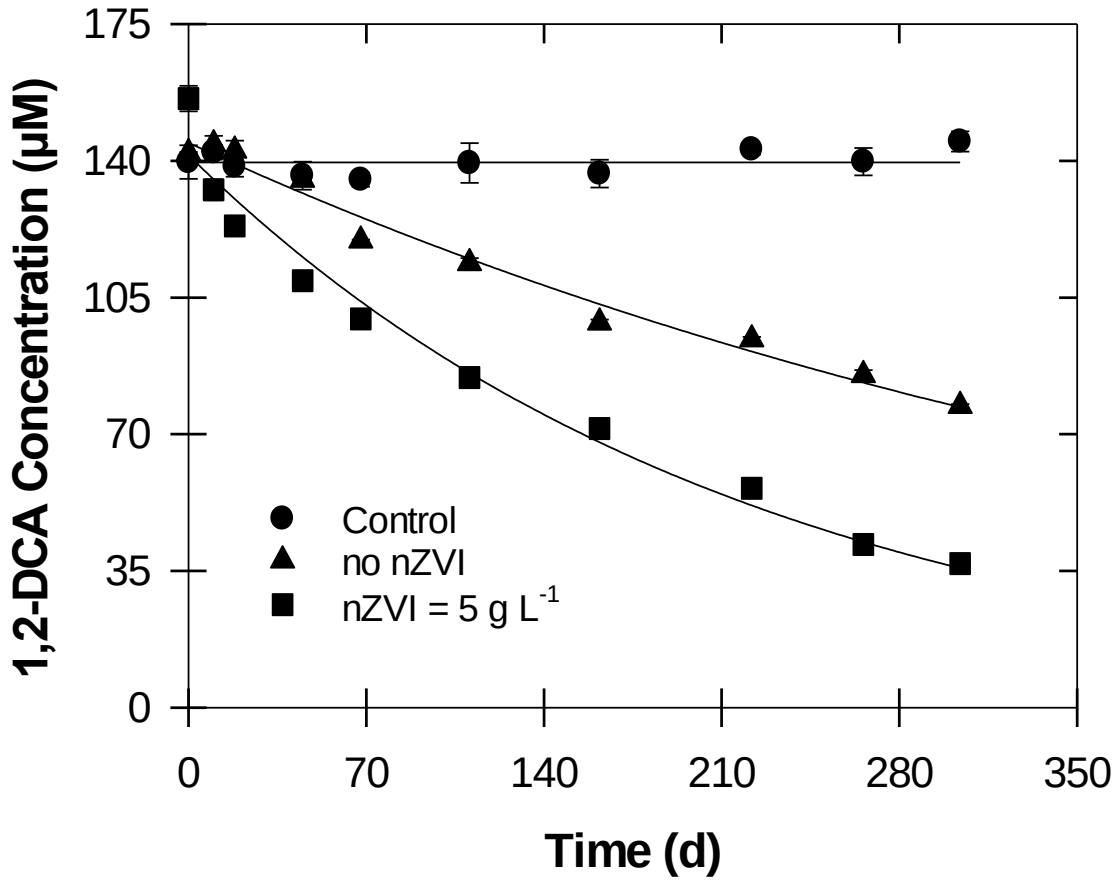

Figure 3.3 Effect of nZVI on 1,2-DCA degradation. Lines are pseudo-first order fittings of data points. In some cases, error bars are smaller than the symbols.

The pseudo-first order rate constant of the dithionite + nZVI (4.5×10^{-3} d^{-1}) treatment is twice that of only dithionite (2.1×10^{-3} d^{-1}). Liu et al. (2012) reported an increase in the reaction rate of dithionite when combined with alumina for the dechlorination of propachlor. The higher reaction rate was attributed to the density of Lewis Acid Sites (LASs) on alumina surfaces. The LASs on alumina can provide active sites for dithionite to form Al-S complexes, which will enhance propachlor degradation (Liu et al., 2012). In the same way, the formation of Fe-S complexes on

the surface of nZVI in this study might increase the reaction rate of the system by facilitating electron transport from the iron core (Kim et al., 2011).

Decreasing nZVI concentration to 2.5 g/L (Exp. 8) (Figure A1) shows that a two-fold decrease in nZVI does not negatively affect the reaction rate of the system (5.3×10^{-3} d^{-1}).

3.3.3. Effect of CMC

Carboxymethyl Cellulose (CMC) is commonly used as a stabilizer to prevent agglomeration of the nanoparticles (He and Zhao, 2008). Though a stabilizer is added primarily to increase the mobility of nZVI in the subsurface, pre-synthesis stabilization with CMC has also shown to enhance its reactivity by increasing the specific surface area of iron (Sakulchaicharoen et al., 2010). CMC can also block reactive surface sites on nZVI and induce chlorinated solvent partitioning to the polymer (Phenrat et al., 2009).

To evaluate the effect of CMC on reactivity, an experiment with 5 g L^{-1} un-stabilized nZVI (i.e., bare-nZVI), 0.5% w/w Pd and 22 mM dithionite was conducted. The CMC-nZVI (Exp. 3) was not as reactive as the bare-nZVI treatment (Exp. 4) (Figure 3.4). The bare-nZVI treatment degraded 92 % of 123 μM 1,2-DCA in 334 days, with an observed pseudo-first order rate constant (k_{obs}) of 7.8×10^{-3} day^{-1}, almost double than that of CMC-nZVI ($k_{obs} = 4.3 \times 10^{-3}$ day^{-1}).

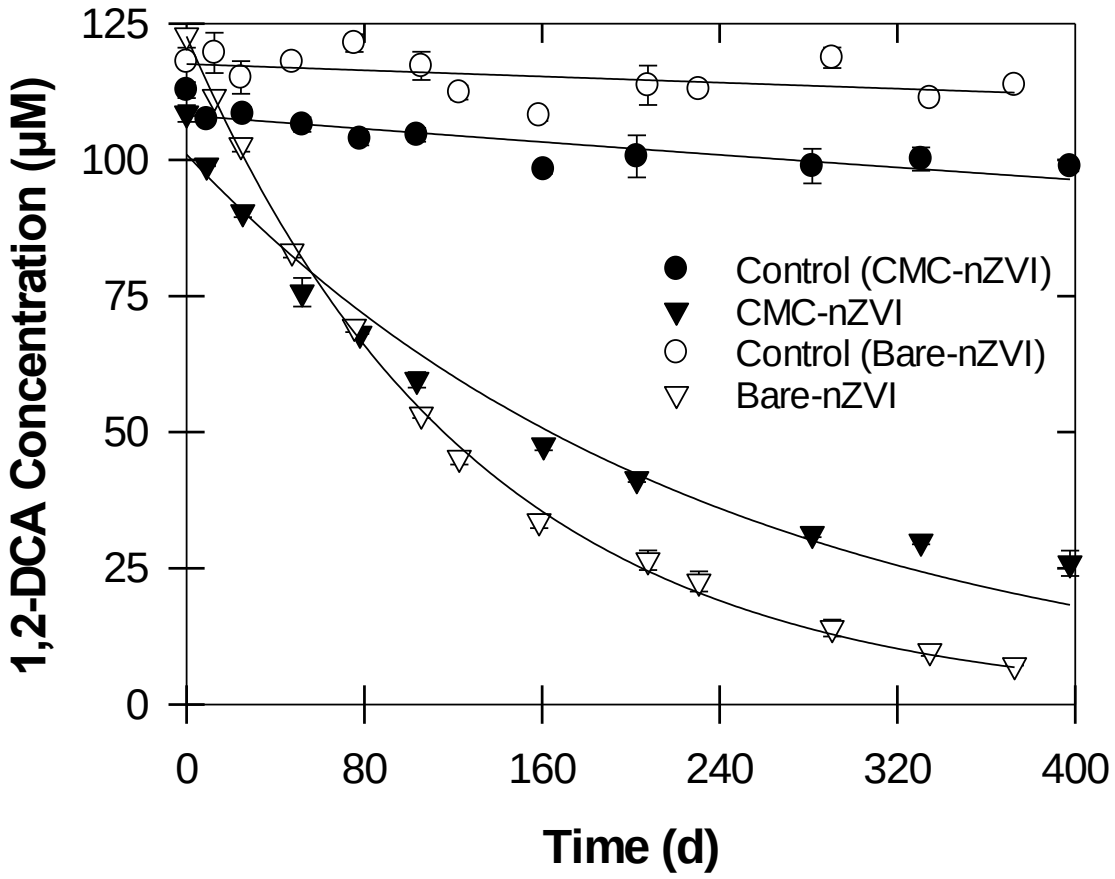

Figure 3.4 Effect of CMC on 1,2-DCA degradation using nZVI (5 g L^{-1}) + dithionite (22 mM). Lines are pseudo-first order fittings of data points. In some cases, error bars are smaller than the symbols.

These results show that the bare nZVI/dithionite formulation is more reactive than CMC stabilized nZVI. Ellis and Little (1986) found that dissolving sodium dithionite in a carboxymethyl cellulose solution significantly decreases its stability. It is possible that CMC is accelerating the decomposition of dithionite. This will favor the formation of less reactive sulfur species (such as thiosulfate and sulfite) than sulphoxyl radicals, which would negatively affect the reactivity. However, to enhance subsurface transport to the contaminated zone the addition of a stabilizer is recommended. Other polymers, such as guar gum, yield physically stable iron

nanoparticles (Sakulchaicharoen et al., 2010) and increase the chemical stability of sodium dithionite (Ellis and Little, 1986). As such alternate stabilizers could be considered for future field applications.

3.3.4. Effect of Palladium

Palladium is used as a catalyst for the dissociation of hydrogen (H_2) derived from the oxidation of iron by water (Equation 3.2) (Wang and Zhang, 1997, Li et al., 2006). Atomic hydrogen can then be used for the hydrodechlorination of chlorinated compounds, increasing the reactivity of nZVI solutions (Liu et al., 2005). Palladium, however, is very sensitive to sulfur poisoning (Kulishkin and Mashkina, 1991). Given dithionite in solution, palladium catalytic function could be negatively impacted. To investigate the impact of dithionite on palladium catalytic function, an experiment without palladium, but with the same nZVI formulation as Exp. 3, was conducted. The reactivity of monometallic nZVI (Exp. 6) towards 1,2-DCA is nearly identical to that with bimetallic nZVI in the presence of dithionite (Figure 3.5). The pseudo-first order rate constants (k_{obs}) of both types of iron are similar (i.e., 4.5 X 10^{-3} d^{-1} for monometallic iron and 4.3 X 10^{-3} d^{-1} for bimetallic iron).

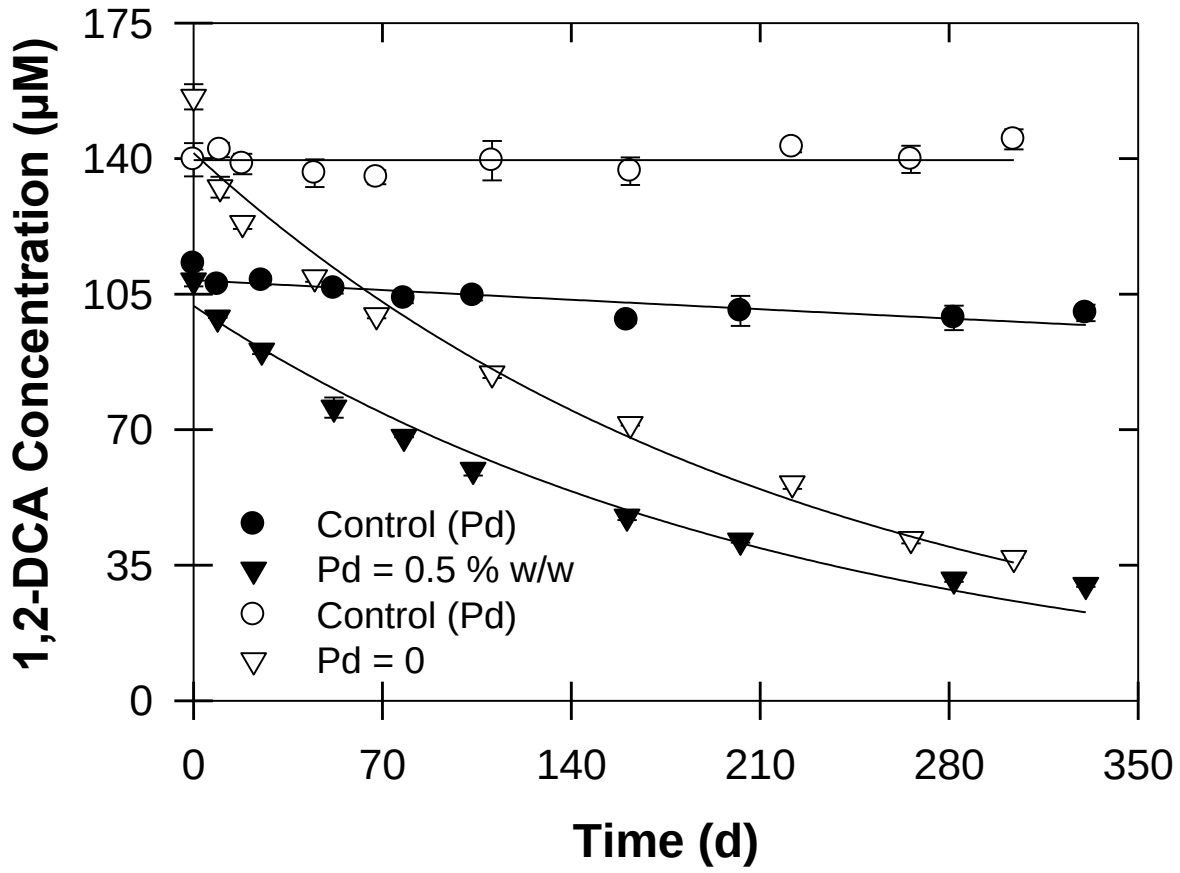

Figure 3.5 Effect of Pd on 1,2-DCA degradation by nZVI (5 g L^{-1}) + dithionite (22 mM). Lines are pseudo-first order fittings of data points. In some cases, error bars are smaller than the symbols.

Comparison of the monometallic and bimetallic nZVI reactivity shows that the presence of palladium does not affect the dechlorination rate. To further assess the extent of palladium poisoning and confirm its inactivity, an analysis of dechlorination products is necessary. Use of palladium as a catalyst for the dechlorination of chlorinated ethenes and ethanes results in degradation products consisting predominantly of fully saturated hydrocarbons (Lien and Zhang, 2001, Lien and Zhang, 2005, He and Zhao, 2008, O'Carroll et al., 2013). The chlorinated hydrocarbons would be degraded through the following pathways: sequential hydrogenolysis or

β-elimination followed by hydrodechlorination. On the other hand, chlorinated ethanes treated with nZVI not doped with palladium will yield degradation products of lesser chlorinated compounds or unsaturated hydrocarbons, with β-elimination as the major pathway (Song and Carraway, 2005).

Due to the slow dechlorination rate of 1,2-DCA, 1,1,2-Trichloroethane (1,1,2-TCA) was chosen as a model contaminant for the analysis of the degradation products. This compound was chosen because it is less recalcitrant than 1,2-DCA and will allow for a faster analysis of its dechlorination products. If palladium is being used as a catalyst the major end product would be ethane, following β-elimination and hydrogenation or sequential hydrogenolysis as reaction pathways. On the other hand, if the reaction is governed mainly by electron transfer following an elimination reaction, the expected end product is vinyl chloride (VC), with β-elimination as the dominant pathway. Note that, in the absence of Pd, zero-valent iron synthesized with borohydride also has the potential to yield saturated hydrocarbons (e.g., ethane) as end products from TCE and 1,1,2-TCA dechlorination (Liu et al., 2005, Song and Carraway, 2005).

Four different treatments with 1,1,2-TCA concentration ranging from 850 to 900 mM and 5 g L^{-1} nZVI in 1% CMC (w/v %) were tested in order to determine the reaction mechanism. For bimetallic nZVI without dithionite complete degradation was achieved after 14 days following consecutive hydrogenolysis, with ethane as the major product (data for ethane not shown) (Figure 3.6). The fast reactivity of this treatment (3.3×10^{-1} d^{-1}) is attributable to the high palladium concentration employed. In contrast, the monometallic nZVI treatment without dithionite was stopped due to excessive hydrogen production (Eq. 3.1 and Eq. 3.2).

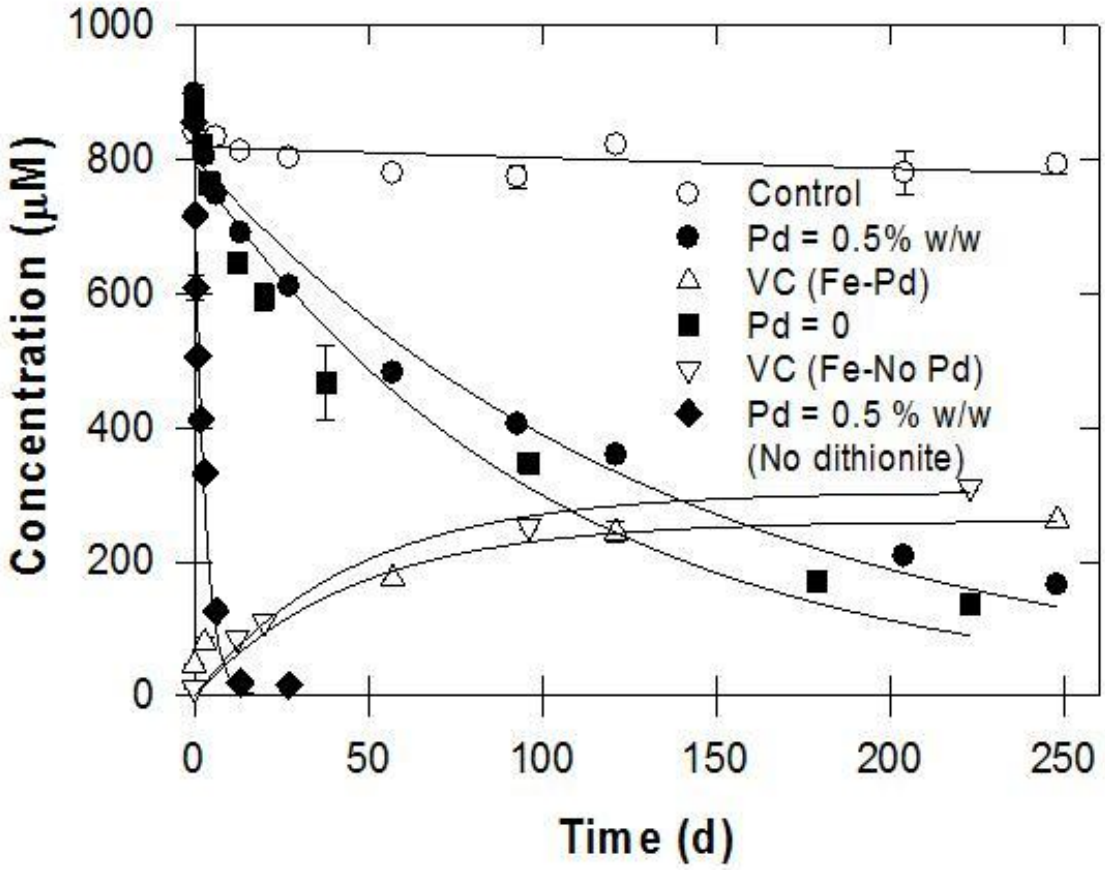

Figure 3.6 Effect of Dithionite on 1,1,2-TCA degradation: 5 g L^{-1} nZVI + 1 % w/v CMC + 22 mM Dithionite (when applicable). Symbols represent average concentrations from duplicate reactors or controls. Lines are pseudo-first order fittings of data points. In some cases, error bars are smaller than the symbols

The last two treatments included 22 mM dithionite, one with 0.5 % w/w Pd (Exp. 12) and one without palladium (Exp. 13) (Figure 3.6). For both cases the major degradation product is vinyl chloride. A comparison between these treatments reveals that the presence of palladium has no effect on the dechlorination of 1,1,2-TCA, achieving the same dechlorination by-products and similar degradation rates (7.3×10^{-3} d^{-1} and 9.7×10^{-3} d^{-1} for bimetallic and monometallic nZVI, respectively). The products indicate that even in the presence of palladium, β-elimination is the

predominant pathway. It also has to be noted that in all the experiments with dithionite, no hydrogen has been observed. This could be due to the consumption of hydrogen by the sulfur compounds derived from dithionite or by the inhibition of the oxidation of nZVI by water. The lack of hydrogen in the system suggests that palladium is not necessary in the present treatment.

3.3.5. Characterization of Iron Nanoparticles

Sodium dithionite has been extensively used for the dissolution of iron oxides from clay minerals (Varadachari et al., 2006). In such reactions, formation of iron sulfides have been observed and attributed to the reaction between Fe^{2+} and hydrogen sulfide (H_2S). Hydrogen sulfide is considered a transient phase in dithionite solutions, which can occur by the following side reactions (Equations 3.10 – 3.11) (Varadachari et al., 2006).

$HS_2O_4^- + H_2O \rightarrow HSO_2^- + HSO_3^- + H^+$ Eq. 3.10

$3HSO_2^- + H^+ \rightarrow H_2S + 2HSO_3^-$ Eq. 3.11

The formation and stability of FeS is favored at high pH, whereas in acidic solutions (pH < 7) dissolution is predominant (Varadachari et al., 2006). Deposition of iron sulfides on the surface of nZVI, in the presence of dithionite, has been reported (Equations 3.12 – 3.14) (Xie and Cwiertny, 2010, Kim et al., 2011). Other researchers have also reported the formation and precipitation of iron sulfides after exposing zero valent iron to different sulfide precursors (e.g., Na_2S and NaHS) (Hassan, 2000, Fan et al., 2013).

$S_2O_4^{2-} + S_2O_3^{2-} + 2H_2O + H^+ \rightarrow H_2S + 3HSO_3$ Eq. 3.12

$H_2S \leftrightarrow S^{2-} + 2H^+$ Eq. 3.13

$Fe^{2+} + S^{2-} \rightarrow FeS$ Eq. 3.14

It is possible that oxidized iron species (e.g., dissolved Fe^{2+} and iron oxides) formed on the surface of nZVI react with dithionite and its decomposition products to form iron sulfides ($Fe_{1-\chi}S$

or $Fe_{1+\chi}S$). To elucidate the reactions taking place between nZVI and dithionite, characterization of three different iron nanoparticles was performed using X-ray Photoelectron Spectroscopy (XPS), X-ray Diffraction (XRD), and Scanning Electron Microscopy (SEM) with Energy Dispersive X-ray (EDX). To assess the changes in the nanoparticles over time, the bare-nZVI/dithionite treatment (Exp. 4) was stopped at 400 days and compared to fresh nZVI/dithionite nanoparticles left to react for 30 minutes and subsequently collected and dried under vacuum. A sample of fresh nZVI (i.e., no dithionite) was also synthesized and collected in a similar manner to evaluate the effect of dithionite on iron surface chemistry and morphology. The fresh nZVI particles were also doped with 0.5 % w/w Pd to better represent the formulations used in the reactivity experiments. Therefore, slight oxidation of fresh particles through reaction with Pd might have occurred following Equation 3.7.

3.3.6. X-ray Diffraction Spectroscopy

XRD analysis was performed to determine the structure of the iron samples (Figure 3.7).

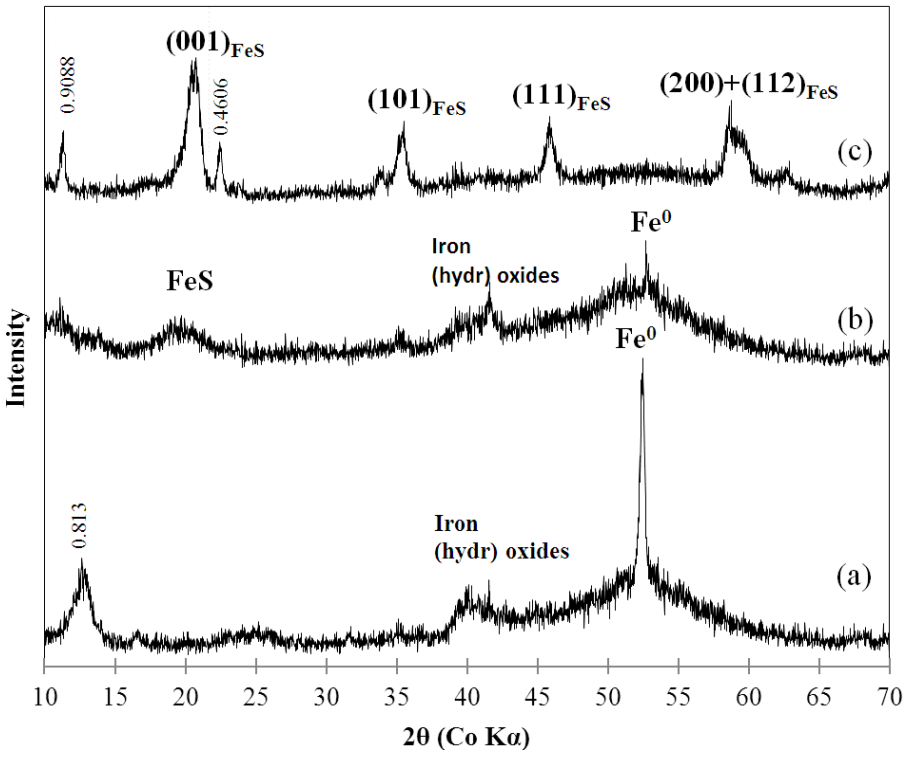

Figure 3.7 XRD patterns of: (a) Freshly synthesized nZVI + Pd (F-1); (b) Freshly synthesized nZVI + Pd + 22 mM Dithionite (F-2); (c) 400 days old nZVI + Pd + 22 mM Dithionite (Exp. 4).

The freshly prepared nZVI displays the characteristic peak of zero valent iron at 52.5° and a broader peak between 39° and 42°, attributable to iron (oxy)(hydr)oxides (Sun et al., 2006, Zhong et al., 2006, Boparai et al., 2010, Siskova et al., 2013) (Figure 3.7a). There is a broad diffraction line at 12.66° with a d-spacing of 0.813 nm, similar to the mineral coquimbite ($Fe_2(SO_4)_3 \cdot 9(H_2O)$) (Barthelmy, 2014a). Formation of sulfur minerals might be a result of the reaction of iron with the sulfur coming from ferrous sulphate, the iron precursor utilized in the

synthesis of nZVI. The fresh nZVI treated with dithionite also shows a distinguishable peak for zero valent iron and iron (oxy)(hydr)oxides, but with a lower intensity (Figure 3.7b). The weak and broad peak at 20° suggest that iron sulfides have started to form (Jeong et al., 2008, Csakberenyi-Malasics et al., 2012, Fan et al., 2013) shortly (within 30 minutes) after injection of dithionite to the nZVI. It is expected that the amorphous phase of mackinawite (also known as disordered mackinawite or amorphous iron(II) monosulfide, FeS_{am}) will form first since it is the first iron sulfide formed through the reaction of Fe^{2+} and S^{2-} (He et al., 2010b). Xie and Cwiertny (2010) treated a partially oxidized nZVI sample with dithionite for 24 hours and even though a fully crystalline phase of iron sulfide was not present, a major diffraction line attributed to mackinawite was observed. Sulfidation of pristine nZVI by Na_2S resulted in the formation of poorly crystalline mackinawite after one day of exposure (Fan et al., 2013). This was also observed in the case of the fresh nZVI/dithionite nanoparticles in this study, indicating the poorly ordered structure of the freshly precipitated iron sulfide. The XRD pattern for the 400 days old nZVI in the current study shows the characteristic peaks of mackinawite with d-spacings similar to those previously reported for synthetic mackinawite (Figure 3.7c, Table 3.2 and Figure B4) (Jeong et al., 2008). It has been suggested that a higher degree of crystallization will occur as the aging time of mackinawite increases (Jeong et al., 2008, Csakberenyi-Malasics et al., 2012). The diffraction line at 11.36° has a d-spacing of 0.9088 nm, which is approximately the same as the d-spacing for ferricopiapite [nominally $Fe_{4.67}(SO_4)_6(OH)_2(H_2O)_{20}$], a mineral formed from the oxidation of iron sulfides (Majzlan and Kiefer, 2006, Majzlan et al., 2006, Barthelmy, 2014b). There is also an unknown diffraction line at 22.44°, with a d-spacing of 0.4606 nm.

Table 3.2 Lattice Spacings for Mackinawite

hkl	This study[a] d (Å)	Jeong et al. (2008)[b] d (Å)	Lennie et al. (1995)[c] d (Å)
001	5.004	5.196	5.0328
101	2.943	2.989	2.9672
111	2.301	2.323	2.3082
200	-	1.845	1.8368
	1.831[a*]		
112	-	1.809	1.8074

a Calculations done using Bragg's Law only for peaks (001), (101), (111), & (200) + (112)

a* Planes (200) & (112) overlap (See Figure 3.7)

b Synthetic mackinawite aged for 3 days

c Well-crystalline mackinawite

Aqueous aging experiments of FeS_{am} have shown that after ~10 months, amorphous mackinawite is completely converted to greigite crystals (Csakberenyi-Malasics et al., 2012). FeS_{am} is metastable and prone to oxidation by sulfur to greigite (Fe_3S_4) and pyrite (FeS_2) (Equation 3.15 - 3.16) (He et al., 2010b):

$$3FeS_{(s)} + S^0_{(s)} \rightarrow Fe_3S_4 \qquad \text{Eq. 3.15}$$

$$FeS_{(s)} + S^0_{(s)} \rightarrow FeS_{2(s)} \qquad \text{Eq. 3.16}$$

In this study, the persistence of mackinawite in solution even after 400 days of reaction suggests that the strong reducing conditions of the system help preserve the reduced iron sulfide phase. These results confirm crystalline iron sulfide species are being formed in solution following the reaction between dithionite and iron, in accordance with XPS analysis (see Section 3.3.7). Iron sulfides on the surface of nZVI can enhance the reductive dechlorination of 1,2-DCA by facilitating the conduction of electrons from the iron core (Kim et al., 2011). Hence, this iron specie might also be contributing to the dechlorination of 1,2-DCA.

3.3.7. X-ray Photoelectron Spectroscopy

Surface analysis of the iron nanoparticles was performed using XPS. Survey spectrum of the fresh and 400 days old nZVI/dithionite particles reveals that the elemental composition of the surface is comprised mainly of iron, boron, carbon, oxygen and sulfur (Figure B1). The fresh nZVI particles have the same composition, with the exception of sulfur (Table B1). Boron comes from the oxidation of borohydride during the synthesis process (Boparai et al., 2013). A small percentage of Pd and sodium (Na) coming from the potassium hexachloropalladate solution dissolved in NaCl is also detected (Figure B2 for HR-XPS spectra of Pd). Fresh nZVI shows the two main peaks for Pd^0 at 335.13 eV and 340.46 eV (Matsumoto et al., 1980, Muftikian et al., 1996, Yan et al., 2010). For fresh and 400 days old nZVI-dithionite, Pd peaks shifted slightly, with the $3d_{5/2}$ peak positioned close to that previously reported for palladium sulfide (PdS) (Table B2) (Matsumoto et al., 1980). The presence of PdS suggests that palladium is being poisoned by sulfur (Kulishkin and Mashkina, 1991). This helps explain the lack of reactivity of palladium observed in the reactivity experiments presented in Section 3.3.4.

Silica (1.2 %) is present only in the old nZVI/dithionite particles, which could be part of the impurities of the sodium dithionite (assay = 88 %) employed. These results are consistent with the data obtained by Energy Dispersive X-ray (EDX) analysis (Figure B3 and Table B3).

Figure 3.8 shows the spectral region of Fe 2p. For fresh nZVI (Figure 3.8a), the peaks at ~706.5 eV and ~719.4 eV correspond to the $2p_{3/2}$ and $2p_{1/2}$ doublet pair of metallic iron (Fe^0), respectively (Grosvenor et al., 2004c). For nZVI-dithionite nanoparticles (Figure 3.8b and 3.8c), these peaks corresponds to both Fe^0 and Fe(II)-S compounds (Mullet et al., 2002, Grosvenor et al., 2004c). Compared to fresh nZVI, peaks with higher intensity at ~706.5 eV are observed in the nZVI-dithionite nanoparticles (fresh and 400 days old), which could be due to the contribution of Fe(II)-S compounds. The proximity of the binding energies for Fe^0 and Fe(II)-S complicates their identification and quantification. Therefore, a hydrogen evolution test was performed to calculate the percentage of zero valent iron to total iron (Table 3.3).

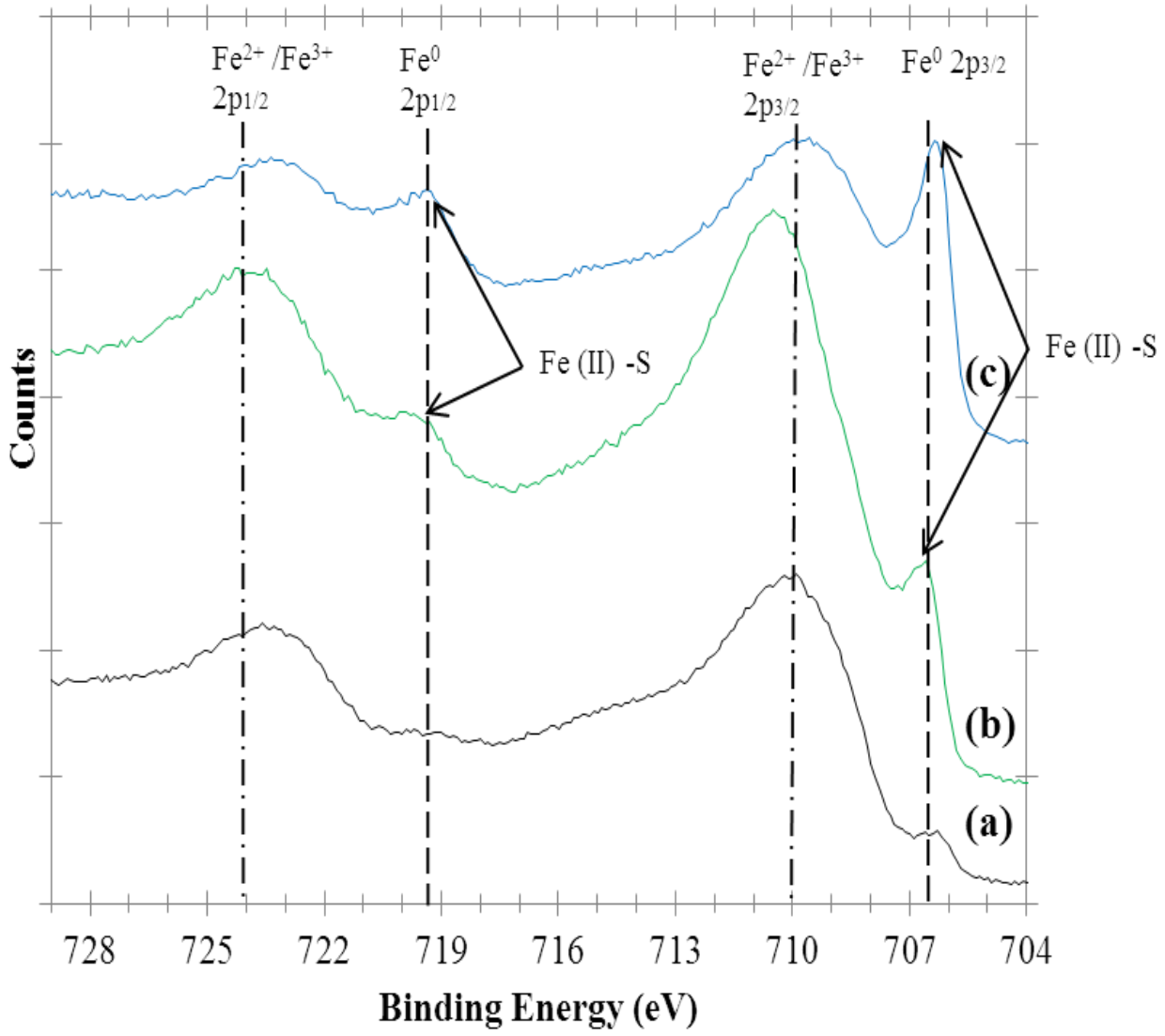

Figure 3.8 High resolution XPS spectra for the Fe 2p region: (a) Fresh nZVI; (b) Fresh nZVI + Dithionite and (c) Old nZVI + Dithionite.

Table 3.3 Percentage of Fe^0 to Total Fe

Treatment	Fresh nZVI	Fresh nZVI + Dithionite	Old nZVI + Dithionite
% Fe^0	82.7	75.7	63

Langell et al. (2009) also reported the photoelectron peak for FeS after reduction of oxidized iron in aquifer sediments by dithionite at alkaline pH. This further supports the formation of FeS after reaction of the nZVI oxide layer with dithionite at the favorable pH (i.e., pH = 8.5). Similarly, the pH of the 400 days old nZVI-dithionite was also high, (8.93 ± 0.07), favorable for the formation of iron sulfides. The Fe $2p_{1/2}$ (~724 eV) and Fe $2p_{3/2}$ (~710 eV) doublet for oxidized iron species (Fe^{2+} and Fe^{3+}) is predominant and indicates that oxidized forms of iron are also present (Grosvenor et al., 2004a). Oxidized iron for these nanoparticles could be present as iron oxides, oxyhydroxides, hydroxides and sulfides, depending on the solution chemistry.

The contribution of iron sulfides to that of the metallic iron peaks located at ~706.5 eV and ~719.4 eV have been qualitatively assessed by evaluating the spectral region for sulfur. For the treatments in which dithionite was added (fresh and old nZVI/dithionite), sulfur is present predominantly as sulfide (Figure 3.9b & 3.9c). The peak for sulfide is located at ~161.5 eV (Mullet et al., 2002) and accounts between 72% and 76% of the total peak area. The peaks for polysulfides, sulphites and sulphates are located at 163, 166.5 and 168.5 eV, respectively (Mullet et al., 2002, Xie and Cwiertny, 2010) and only account for approximately 24% (it must be noted that only the fittings corresponding to S $2p_{3/2}$ are presented in Figure 3.9). In contrast, for the fresh nZVI with no dithionite, no significant sulfur peak was present, with all the sulfur being attributed to sulphate coming from the iron precursor ($FeSO_4 \cdot 7H_2O$) (Figure 3.9a). This indicates that in the presence of dithionite, sulfur is mostly associated with iron sulfides ($Fe_{1+x}S$ or $Fe_{1-x}S$), which is also supported by the XRD results.

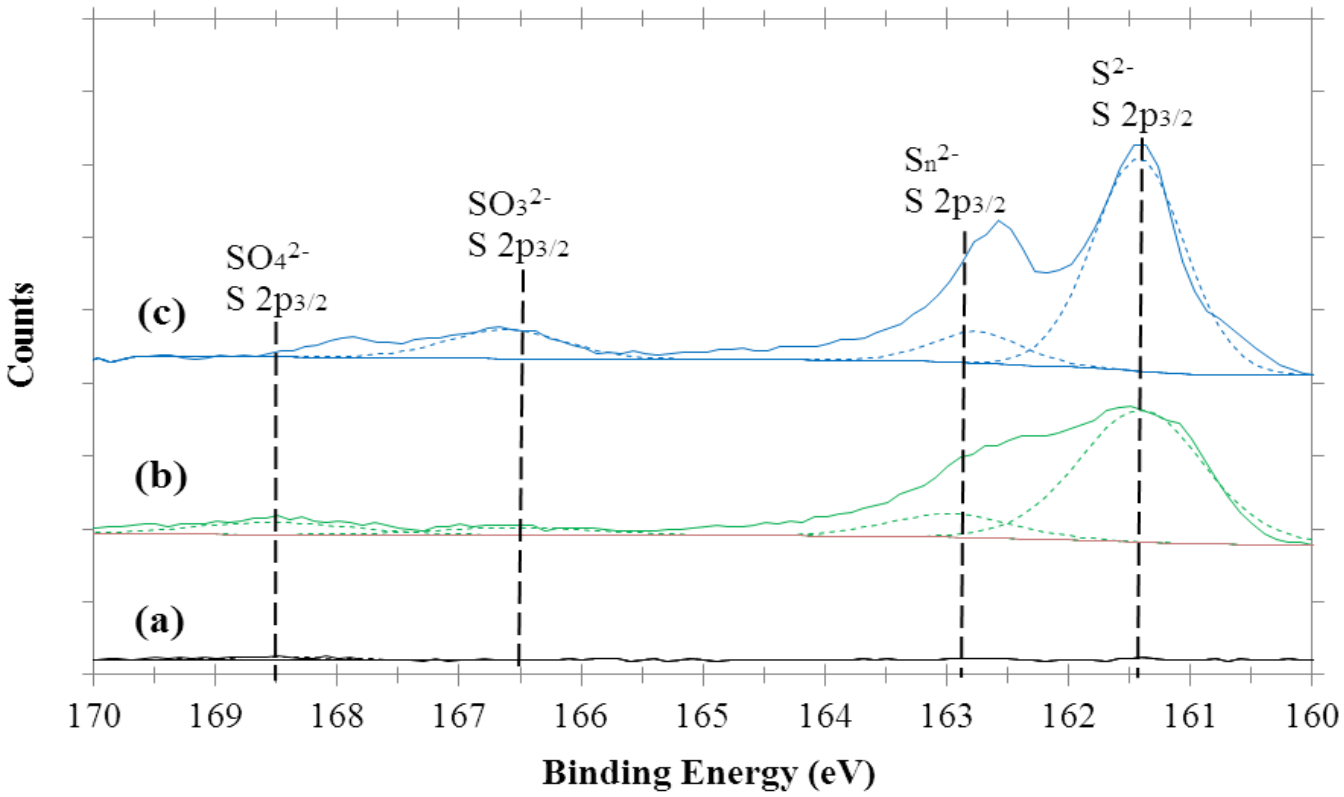

Figure 3.9 High resolution XPS spectra for the S 2p region: (a) Fresh nZVI; (b) Fresh nZVI + Dithionite and (c) Old nZVI + Dithionite.

High resolution spectra of the O 1s region reveals that oxygen is mostly in the form of OH^- (~531.2eV) with 72 to 84% and O^{2-} (~529.7 eV) with 7 to 21% of the total peak area, respectively (Grosvenor et al., 2004b) (Figure 3.10). In the case of fresh and 400 days old nZVI-dithionite (Figure 3.10b and 3.10c), a small percent of oxygen could also be associated with sulfite and sulfate (Figure 3.9b and 3.9c). Oxygen associated with H_2O (~532.6 eV) only accounted for 6 to 10% of the area (Grosvenor et al., 2004b). The predominance of OH^- in nZVI systems has been associated with the presence of iron hydroxides and iron oxyhydroxides (Boparai et al., 2013).

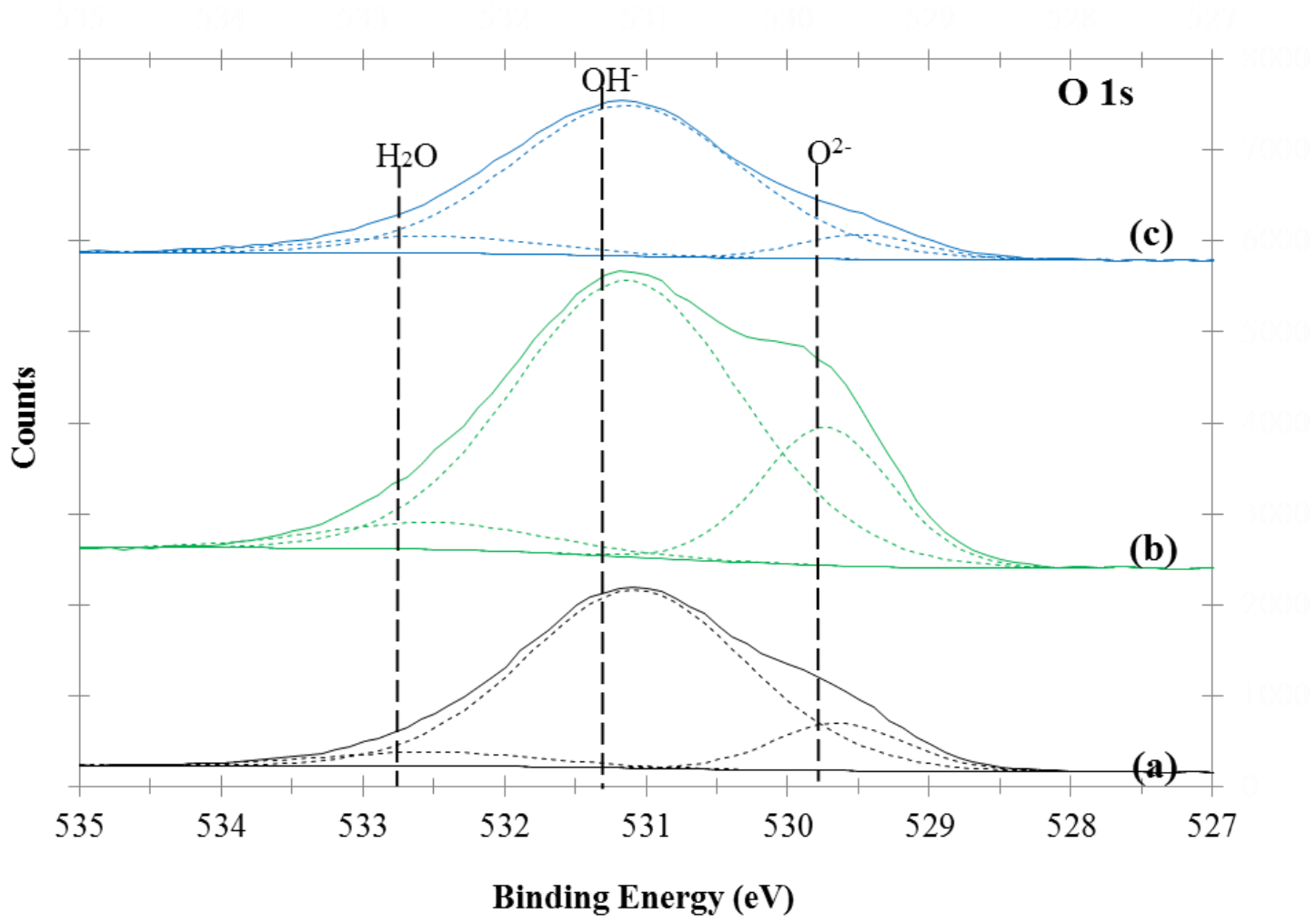

Figure 3.10 High resolution XPS spectra for the O 1s region: (a) Fresh nZVI; (b) Fresh nZVI + Dithionite and (c) Old nZVI + Dithionite.

3.3.8. Scanning Electron Microscopy

SEM analysis of fresh nZVI (with no dithionite) particles shows that the nZVI particles are comprised of individual, spherical particles forming chains and aggregates due to magnetic interactions (Figure 3.11a). Some larger plate-like structures are also present (Figure 3.11a), possibly from iron (oxy)(hydr)oxides formation during Pd reduction. In Figure 3.11b, curved and wrinkled sheets attributed to FeS_{am} can also be distinguished (Csakberenyi-Malasics et al.,

2012). Figure 3.11c shows that for the 400 days old sample spherical nanoparticles are still visible, but with the predominant presence of the FeS_{am} platelets sheets.

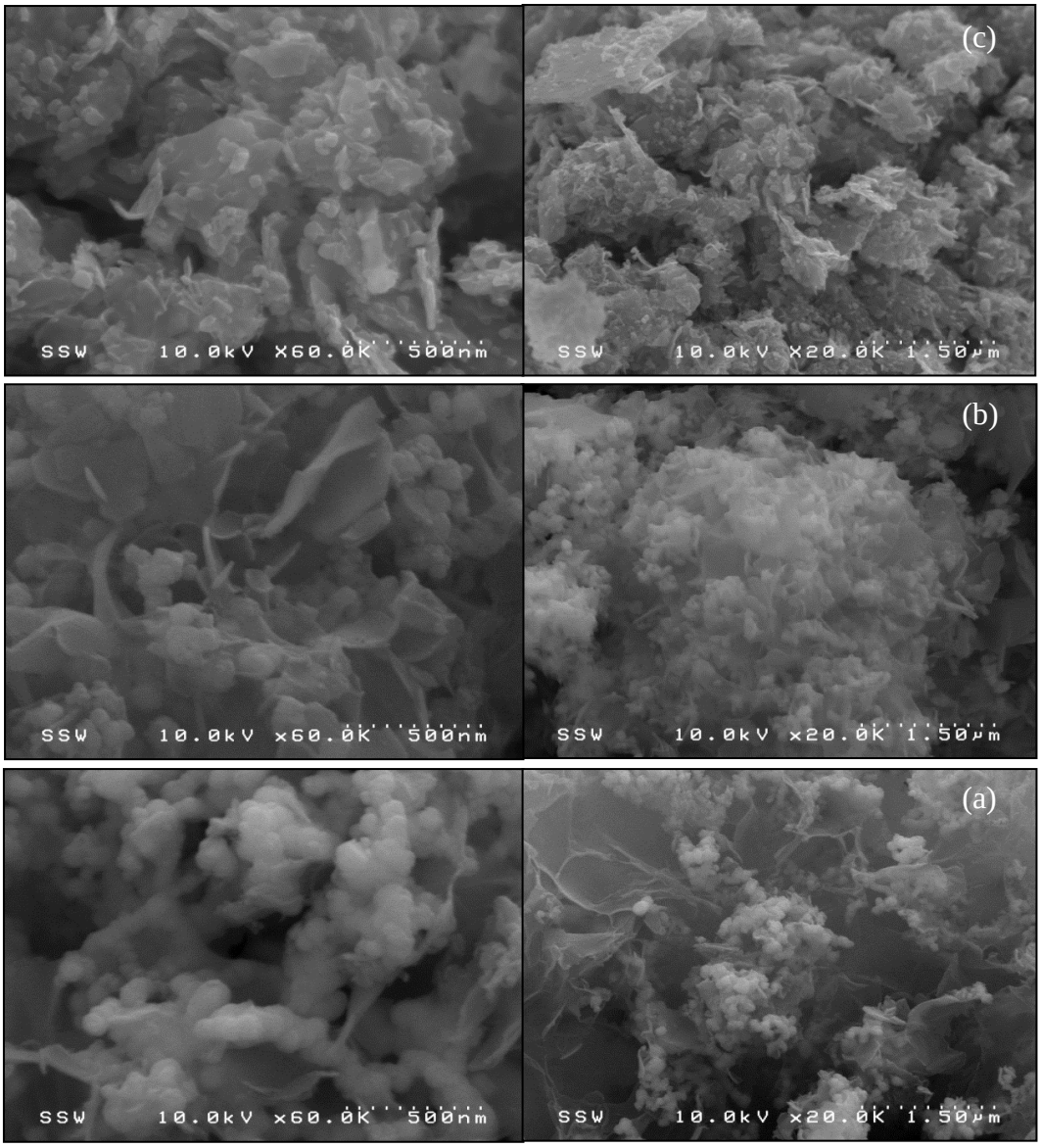

Figure 3.11 SEM images of: (a) Fresh nZVI; (b) Fresh nZVI + Dithionite and (c) Old nZVI + Dithionite.

3.3.9. Discussion

XPS and hydrogen test (Table 3.3) results for the 400 days old nZVI/dithionite particles confirm the persistence of zero valent iron in solution, even after one year of reactivity (Figure 3.4). The presence of zero valent iron suggests that iron is not being oxidized by water (Eq. 3.1), as was noted in Section 3.3.4. By providing strong reducing conditions, dithionite could be inhibiting the oxidation of nZVI by water, thus, resulting in the conservation of zero valent iron. This would also reduce the formation of hydrogen, which has not been observed in any reactivity experiments involving nZVI and dithionite. In the same way, dithionite could also serve as a scavenger for electron accepting compounds in solution (e.g., O_2), which would help preserve zero valent iron.

Based on XPS and XRD results presented above, it is proposed that upon addition of dithionite to the oxidized iron in Exp. 2, iron sulfides are being formed. These iron sulfides in the presence of dithionite are capable of dechlorinating 1,2-DCA, as confirmed by the iron sulfide/dithionite experiment (Exp. 10).

3.4. Conclusions

The present research work has shown that an nZVI/Dithionite formulation is capable of abiotically dechlorinating 1,2-DCA. Characterization analysis of the iron nanoparticles used in reactivity experiments shows that in the presence of dithionite, zero valent iron as such remained in solution for more than a year. This represent unprecedented lifetime for the type of nZVI used in this research work. This shows that as a new nZVI-amendment for in situ remediation, dithionite helps overcome limitations associated with the zero valent iron technology, such as

short reactive lifetime. It was found that the addition of palladium to the nZVI is not necessary for 1,2-DCA dechlorination using the nZVI/Dithionite treatment. This reduces the complexity and cost associated with nZVI for field applications. Product analysis using 1,1,2-TCA shows β-elimination as the main degradation pathway for the dechlorination of this compound. This suggests that for the reactions with chlorinated ethanes, reductive dechlorination may be the main dechlorination pathway.

Similar reaction rates to the one achieved using an nZVI/dithionite formulation was achieved by combining iron sulfide and magnetite with dithionite. The later iron species were previously considered unreactive towards 1,2-DCA (iron sulfide) or poor reductants for dechlorination of organic compounds (magnetite). In the same way, a homogenous solution ofdithionite was capable of dechlorinating 1,2-DCA, with reaction rates in the same order of magnitude to the heterogeneous dithionite solution. This finding shows that dithionite can also be used alone or with other iron species for effective dechlorination of recalcitrant chlorinated compounds, expanding in this way its application.

To date, no research using nZVI has been able to abiotically degrade 1,2-DCA. Similarly, the used of dithionite in the field had been limited to sites with sufficient dithionite-reducible iron (e.g., Fe^{2+}). Thus, the development of dithionite-nanometal based formulation capable of abiotically degrading 1,2-DCA that can be safely implemented in the field represents an important breakthrough.

3.5. References

Amonette, J. E., J. E. Szecsody, H. T. Schaef, Y. A. Gorby, J. S. Fruchter and J. C. Templeton (1994). Abiotic reduction of aquifer materials by dithionite: A promising in-situ remediation technology. Conference: 33. Hanford symposium on health and the environment: symposium on in-situ remediation--scientific basis for current and future technologies, Richland, WA (United States), 7-11 Nov 1994; Other Information: PBD: Nov 1994**:** Medium: ED; Size: 53 p.

Arnold, W. A., W. P. Ball and A. L. Roberts (1999). "Polychlorinated ethane reaction with zero-valent zinc: pathways and rate control." Journal of Contaminant Hydrology **40**(2): 183-200.

ATSDR (2001). Toxicological Profile for 1,2-Dichloroethane. Public Health Service. U. S. D. o. H. a. H. Services. Atlanta, GA.

Barthelmy, D. (2014a). "Coquimbite Mineral Data." Retrieved September 2, 2014, 2014, from http://webmineral.com/data/Coquimbite.shtml#.VAY7mMVdXuR.

Barthelmy, D. (2014b). "Ferricopiapite Mineral Data." Retrieved Spetermber 2, 2014, 2014, from http://webmineral.com/data/Ferricopiapite.shtml#.VAYlc8VdXuQ.

Boparai, H. K., S. D. Comfort, T. Satapanajaru, J. E. Szecsody, P. R. Grossl and P. J. Shea (2010). "Abiotic transformation of high explosives by freshly precipitated iron minerals in aqueous Fe-II solutions." Chemosphere **79**(8): 865-872.

Boparai, H. K., S. D. Comfort, P. J. Shea and J. E. Szecsody (2008). "Remediating explosive-contaminated groundwater by in situ redox manipulation (ISRM) of aquifer sediments." Chemosphere **71**(5): 933-941.

Boparai, H. K., M. Joseph and D. M. O'Carroll (2013). "Cadmium (Cd2+) removal by nano zerovalent iron: surface analysis, effects of solution chemistry and surface complexation modeling." Environmental Science and Pollution Research **20**(9): 6210-6221.

Boparai, H. K., P. J. Shea, S. D. Comfort and D. D. Snow (2006). "Dechlorinating chloroacetanilide herbicides by dithionite-treated aquifer sediment and surface soil." Environmental Science & Technology **40**(9): 3043-3049.

Butler, E. C. and K. F. Hayes (1998). "Effects of Solution Composition and pH on the Reductive Dechlorination of Hexachloroethane by Iron Sulfide." Environmental Science & Technology **32**(9): 1276-1284.

Butler, E. C. and K. F. Hayes (2000). "Kinetics of the transformation of halogenated aliphatic compounds by iron sulfide." Environmental Science & Technology **34**(3): 422-429.

Castillo, R. M., V. A. Nzengung and G. L. Mills (1997). "Enhanced degradation of tetrachloroethylene by redox manipulated iron-bearing clays and aquifer materials." Abstracts of Papers of the American Chemical Society **213**: 186-ENVR.

Csakberenyi-Malasics, D., J. D. Rodriguez-Blanco, V. K. Kis, A. Recnik, L. G. Benning and M. Posfai (2012). "Structural properties and transformations of precipitated FeS." Chemical Geology **294**: 249-258.

Daida, E. J. and J. C. Peters (2004). "Considering Fe-II/IV redox processes as mechanistically relevant to the catalytic hydrogenation of olefins by [PhBp(iPr)3]Fe-H-x species." Inorganic Chemistry **43**(23): 7474-7485.

de Boer, C. V. (2012). Transport of Nano Sized Zero Valent Iron Colloids during Injection into the Subsurface. Doctor of Philosophy, Universitat Stuttgart.

De Wildeman, S., G. Linthout, H. Van Langenhove and W. Verstraete (2004). "Complete lab-scale detoxification of groundwater containing 1,2-dichloroethane." Applied Microbiology and Biotechnology **63**(5): 609-612.

De Wildeman, S. and W. Verstraete (2003). "The quest for microbial reductive dechlorination of C-2 to C-4 chloroalkanes is warranted." Applied Microbiology and Biotechnology **61**(2): 94-102.

Ellis, L. C. and E. D. Little (1986). Stabilized Dithionite Solutions. U. S. Patent. United States**:** 3.

Fairley, N. (1999). "CasaXPS Version 2.3.14." from http://www.casaxps.com/.

Fan, D. M., R. P. Anitori, B. M. Tebo, P. G. Tratnyek, J. S. L. Pacheco, R. K. Kukkadapu, M. H. Engelhard, M. E. Bowden, L. Kovarik and B. W. Arey (2013). "Reductive Sequestration of Pertechnetate ((TcO4-)-Tc-99) by Nano Zerovalent Iron (nZVI) Transformed by Abiotic Sulfide." Environmental Science & Technology **47**(10): 5302-5310.

Feitz, A. J., J. Guan and T. D. Waite (2004). Process for Producing a Nanoscale Zero-Valent Metal. Australia, CRC For Waste Management and Pollution Control Limited.

Filip, J., F. Karlicky, Z. Marusak, P. Lazar, M. Cernik, M. Otyepka and R. Zboril (2014). "Anaerobic Reaction of Nanoscale Zerovalent Iron with Water: Mechanism and Kinetics." Journal of Physical Chemistry C **118**(25): 13817-13825.

Fruchter, J. S., C. R. Cole, M. D. Williams, V. R. Vermeul, J. E. Amonette, J. E. Szecsody, J. D. Istok and M. D. Humphrey (2000). "Creation of a subsurface permeable treatment zone for aqueous chromate contamination using in situ redox manipulation." Ground Water Monitoring and Remediation **20**(2): 66-77.

Fruchter, J. S., F. A. Spane and J. E. Amonette (1994). Interim report: Manipulation of natural subsurface processes: Field research and validation. Other Information: PBD: Nov 1994**:** Medium: ED; Size: 107 p.

Gan, H., J. W. Stucki and G. W. Bailey (1992). "Reduction of Structural Iron in Ferruginous Smectite by Free-Radicals." Clays and Clay Minerals **40**(6): 659-665.

Gillham, R. W. and S. F. Ohannesin (1994). "Enhanced Degradation of Halogenated Aliphatics by Zero-Valent Iron." Ground Water **32**(6): 958-967.

Grosvenor, A. P., B. A. Kobe, M. C. Biesinger and N. S. McIntyre (2004a). "Investigation of multiplet splitting of Fe 2p XPS spectra and bonding in iron compounds." Surface and Interface Analysis **36**(12): 1564-1574.

Grosvenor, A. P., B. A. Kobe and N. S. McIntyre (2004b). "Studies of the oxidation of iron by air after being exposed to water vapour using angle-resolved X-ray photoelectron spectroscopy and QUASES." Surface and Interface Analysis **36**(13): 1637-1641.

Grosvenor, A. P., B. A. Kobe and N. S. McIntyre (2004c). "Studies of the oxidation of iron by water vapour using X-ray photoelectron spectroscopy and QUASES (TM)." Surface Science **572**(2-3): 217-227.

Hassan, S. M. (2000). "Reduction of halogenated hydrocarbons in aqueous media: I. Involvement of sulfur in iron catalysis." Chemosphere **40**(12): 1357-1363.

He, F., D. Zhao and C. Paul (2010a). "Field assessment of carboxymethyl cellulose stabilized iron nanoparticles for in situ destruction of chlorinated solvents in source zones." Water Res **44**(7): 2360-2370.

He, F. and D. Y. Zhao (2005). "Preparation and characterization of a new class of starch-stabilized bimetallic nanoparticles for degradation of chlorinated hydrocarbons in water." Environmental Science & Technology **39**(9): 3314-3320.

He, F. and D. Y. Zhao (2007). "Manipulating the size and dispersibility of zerovalent iron nanoparticles by use of carboxymethyl cellulose stabilizers." Environmental Science & Technology **41**(17): 6216-6221.

He, F. and D. Y. Zhao (2008). "Hydrodechlorination of trichloroethene using stabilized Fe-Pd nanoparticles: Reaction mechanism and effects of stabilizers, catalysts and reaction conditions." Applied Catalysis B-Environmental **84**(3-4): 533-540.

He, Y. T., J. T. Wilson and R. T. Wilkin (2010b). "Impact of iron sulfide transformation on trichloroethylene degradation." Geochimica et Cosmochimica Acta **74**(7): 2025-2039.

Health-Canada (2012). 1,2-Dichloroethane in Drinking Water. F.-P.-T. C. o. D. Water. Ottawa, Ontario.

Huang, C. C., S. L. Lo and H. L. Lien (2012). "Zero-valent copper nanoparticles for effective dechlorination of dichloromethane using sodium borohydride as a reductant." Chemical Engineering Journal **203**: 95-100.

Huang, C. C., S. L. Lo, S. M. Tsai and H. L. Lien (2011). "Catalytic hydrodechlorination of 1,2-dichloroethane using copper nanoparticles under reduction conditions of sodium borohydride." Journal of Environmental Monitoring **13**(9): 2406-2412.

IARC (1999). Monographs on the Evaluation of the Carcinogenic Risk of Chemicals to Humans. Re-evaluation of Some Organic Chemicals, Hydrozine and Hydrogen Peroxide (Part Two). Lyon, World Health Organization. **Vol. 71:** 501-529.

Jeong, H. Y., J. H. Lee and K. F. Hayes (2008). "Characterization of synthetic nanocrystalline mackinawite: Crystal structure, particle size, and specific surface area." Geochimica Et Cosmochimica Acta **72**(2): 493-505.

Kim, E. J., J. H. Kim, A. M. Azad and Y. S. Chang (2011). "Facile Synthesis and Characterization of Fe/FeS Nanoparticles for Environmental Applications." Acs Applied Materials & Interfaces **3**(5): 1457-1462.

Kriegman-King, M. R. and M. Reinhard (1994). "Transformation of Carbon Tetrachloride by Pyrite in Aqueous Solution." Environmental Science & Technology **28**(4): 692-700.

Kulishkin, N. T. and A. V. Mashkina (1991). "Deactivation of Rhodium and Palladium Catalysts by Sulfur-Compounds." Reaction Kinetics and Catalysis Letters **45**(1): 41-47.

Langell, M. A., E. Kadossov, H. Boparai and P. Shea (2009). "Effect of sodium dithionite on the surface composition of iron-containing aquifer sediment." Surface and Interface Analysis **41**(12-13): 941-950.

Le, N. B. and N. V. Coleman (2011). "Biodegradation of vinyl chloride, cis-dichloroethene and 1,2-dichloroethane in the alkene/alkane-oxidising Mycobacterium strain NBB4." Biodegradation **22**(6): 1095-1108.

Lee, W. and B. Batchelor (2002). "Abiotic reductive dechlorination of chlorinated ethylenes by iron-bearing soil minerals. 1. Pyrite and magnetite." Environmental Science & Technology **36**(23): 5147-5154.

Lennie, A. R., S. A. T. Redfern, P. F. Schofield and D. J. Vaughan (1995). "Synthesis and Rietveld crystal structure refinement of mackinawite, tetragonal FeS." Mineralogical Magazine **59**(397): 677-683.

Leussing, D. L. and I. M. Kolthoff (1953). "The Solubility Product of Ferrous Hydroxide and the Ionization of the Aquo-Ferrous Ion." Journal of the American Chemical Society **75**(10): 2476-2479.

Li, X.-q., D. W. Elliott and W.-x. Zhang (2006). "Zero-Valent Iron Nanoparticles for Abatement of Environmental Pollutants: Materials and Engineering Aspects." Critical Reviews in Solid State and Materials Sciences **31**(4): 111-122.

Lien, H. L. and W. X. Zhang (2001). "Nanoscale iron particles for complete reduction of chlorinated ethenes." Colloids and Surfaces a-Physicochemical and Engineering Aspects **191**(1-2): 97-105.

Lien, H. L. and W. X. Zhang (2005). "Hydrodechlorination of chlorinated ethanes by nanoscale Pd/Fe bimetallic particles." Journal of Environmental Engineering-Asce **131**(1): 4-10.

Liu, C. S., K. M. Shih, Y. X. Gao, F. B. Li and L. Wei (2012). "Dechlorinating transformation of propachlor through nucleophilic substitution by dithionite on the surface of alumina." Journal of Soils and Sediments **12**(5): 724-733.

Liu, X., B. P. Vellanki, B. Batchelor and A. Abdel-Wahab (2014). "Degradation of 1,2-dichloroethane with advanced reduction processes (ARPs): Effects of process variables and mechanisms." Chemical Engineering Journal **237**(0): 300-307.

Liu, Y. Q., H. Choi, D. Dionysiou and G. V. Lowry (2005). "Trichloroethene hydrodechlorination in water by highly disordered monometallic nanoiron." Chemistry of Materials **17**(21): 5315-5322.

Lopez, J. A., F. González, F. A. Bonilla, G. Zambrano and M. E. Gómez (2010). SYNTHESIS AND CHARACTERIZATION OF Fe 3 O 4 MAGNETIC NANOFLUID.

Majzlan, J. and B. Kiefer (2006). "An X-ray- and neutron-diffraction study of synthetic ferricopiapite, Fe-14/3(SO4)(6)(OD,OH)(2)(D2O,H2O)(20), and ab initio calculations on the structure of magnesiocopiapite, MgFe4(So(4))(6)(OH)(2)(H2O)(20)." Canadian Mineralogist **44**: 1227-1237.

Majzlan, J., A. Navrotsky, R. B. McCleskey and C. N. Alpers (2006). "Thermodynamic properties and crystal structure refinement of ferricopiapite, coquimbite, rhomboclase, and Fe-2(SO4)(3)(H2O)(5)." European Journal of Mineralogy **18**(2): 175-186.

Makarov, S. V. and R. Silaghi-Dumitrescu (2013). "Sodium dithionite and its relatives: past and present." Journal of Sulfur Chemistry **34**(4): 444-449.

Matheson, L. J. and P. G. Tratnyek (1994). "Reductive Dehalogenation of Chlorinated Methanes by Iron Metal." Environmental Science & Technology **28**(12): 2045-2053.

Matsumoto, Y., M. Soma, T. Onishi and K. Tamaru (1980). "State of Sulfur on the Palladium Surface Studied by Auger-Electron Spectroscopy, Electron-Energy Loss Spectroscopy, Ultraviolet Photoelectron-Spectroscopy and X-Ray Photoelectron-Spectroscopy." Journal of the Chemical Society-Faraday Transactions I **76**: 1122-1130.

Maymo-Gatell, X., T. Anguish and S. H. Zinder (1999). "Reductive dechlorination of chlorinated ethenes and 1,2-dichloroethane by "Dehalococcoides ethenogenes" 195." Applied and Environmental Microbiology **65**(7): 3108-3113.

Moran, M. J., J. S. Zogorski and P. J. Squillace (2006). "Chlorinated Solvents in Groundwater of the United States." Environmental Science & Technology **41**(1): 74-81.

Muftikian, R., K. Nebesny, Q. Fernando and N. Korte (1996). "X-ray photoelectron spectra of the palladium-iron bimetallic surface used for the rapid dechlorination of chlorinated organic environmental contaminants." Environmental Science & Technology **30**(12): 3593-3596.

Muir, S. S. and X. D. Yao (2011). "Progress in sodium borohydride as a hydrogen storage material: Development of hydrolysis catalysts and reaction systems." International Journal of Hydrogen Energy **36**(10): 5983-5997.

Mullet, M., S. Boursiquot, M. Abdelmoula, J. M. Genin and J. J. Ehrhardt (2002). "Surface chemistry and structural properties of mackinawite prepared by reaction of sulfide ions with metallic iron." Geochimica Et Cosmochimica Acta **66**(5): 829-836.

Naftz, D. L., S. J. Morrison, J. A. Davis and C. C. Fuller (2002). Handbook of groundwater remediation using permeable reactive barriers : applications to radionuclides, trace metals, and nutrients. San Diego, CA, San Diego, CA: Academic Press, c2002.

Nurmi, J. T., P. G. Tratnyek, V. Sarathy, D. R. Baer, J. E. Amonette, K. Pecher, C. M. Wang, J. C. Linehan, D. W. Matson, R. L. Penn and M. D. Driessen (2005). "Characterization and properties of metallic iron nanoparticles: Spectroscopy, electrochemistry, and kinetics." Environmental Science & Technology **39**(5): 1221-1230.

Nzengung, V. A., R. M. Castillo, W. P. Gates and G. L. Mills (2001). "Abiotic transformation of perchloroethylene in homogeneous dithionite solution and in suspensions of dithionite-treated clay minerals." Environmental Science & Technology **35**(11): 2244-2251.

O'Carroll, D., B. Sleep, M. Krol, H. Boparai and C. Kocur (2013). "Nanoscale zero valent iron and bimetallic particles for contaminated site remediation." Advances in Water Resources **51**: 104-122.

Phenrat, T., Y. Q. Liu, R. D. Tilton and G. V. Lowry (2009). "Adsorbed Polyelectrolyte Coatings Decrease Fe-0 Nanoparticle Reactivity with TCE in Water: Conceptual Model and Mechanisms." Environmental Science & Technology **43**(5): 1507-1514.

Phenrat, T., N. Saleh, K. Sirk, R. D. Tilton and G. V. Lowry (2007). "Aggregation and sedimentation of aqueous nanoscale zerovalent iron dispersions." Environmental Science & Technology **41**(1): 284-290.

Pyatnitskii, Y. I., I. T. Chashechnikova and N. V. Pavlenko (1996). "Mechanism and kinetics of the hydrogenation of CO with the formation of paraffins and olefins on an iron catalyst." Theoretical and Experimental Chemistry **32(**2): 103-107.

Rodriguez, J. C. and M. Rivera (1997). "Reductive dehalogenation of carbon tetrachloride by sodium dithionite." Chemistry Letters(11): 1133-1134.

Sakulchaicharoen, N., D. M. O'Carroll and J. E. Herrera (2010). "Enhanced stability and dechlorination activity of pre-synthesis stabilized nanoscale FePd particles." J Contam Hydrol **118**(3-4): 117-127.

Saleh, N., K. Sirk, Y. Q. Liu, T. Phenrat, B. Dufour, K. Matyjaszewski, R. D. Tilton and G. V. Lowry (2007). "Surface modifications enhance nanoiron transport and NAPL targeting in saturated porous media." Environmental Engineering Science **24**(1): 45-57.

Schrick, B., B. W. Hydutsky, J. L. Blough and T. E. Mallouk (2004). "Delivery vehicles for zerovalent metal nanoparticles in soil and groundwater." Chemistry of Materials **16**(11): 2187-2193.

Siskova, K. M., L. Machala, J. Tucek, J. Kaslik, P. Mojzes and R. Zboril (2013). "Mixtures of L-Amino Acids as Reaction Medium for Formation of Iron Nanoparticles: The Order of Addition into a Ferrous Salt Solution Matters." International Journal of Molecular Sciences **14**(10): 19452-19473.

Smidt, H. and W. M. de Vos (2004). "Anaerobic microbial dehalogenation." Annual Review of Microbiology **58**: 43-73.

Soesilo, J. A. and S. R. Wilson (1997). Site Remediation Planning and Management. Boca Raton, FL, Lewis Publishers.

Soga, K., J. W. E. Page and T. H. Illangasekare (2004). "A review of NAPL source zone remediation efficiency and the mass flux approach." Journal of Hazardous Materials **110**(1-3): 13-27.

Song, H. and E. R. Carraway (2005). "Reduction of chlorinated ethanes by nanosized zero-valent iron: Kinetics, pathways, and effects of reaction conditions." Environmental Science & Technology **39**(16): 6237-6245.

Stroo, H. F., M. Unger, C. H. Ward, M. C. Kavanaugh, C. Vogel, A. Leeson, J. A. Marqusee and B. P. Smith (2003). "Remediating chlorinated solvent source zones." Environmental Science & Technology **37**(11): 224a-230a.

Sun, Q., A. J. Feitz, J. Guan and T. D. Waite (2008). "COMPARISON OF THE REACTIVITY OF NANOSIZED ZERO-VALENT IRON (nZVI) PARTICLES PRODUCED BY BOROHYDRIDE AND DITHIONITE REDUCTION OF IRON SALTS." Nano **3**(5): 341-349.

Sun, Y. P., X. Q. Li, J. Cao, W. X. Zhang and H. P. Wang (2006). "Characterization of zero-valent iron nanoparticles." Adv Colloid Interface Sci **120**(1-3): 47-56.

Szecsody, J. E., J. S. Fruchter, M. D. Williams, V. R. Vermeul and D. Sklarew (2004). "In situ chemical reduction of aquifer sediments: Enhancement of reactive iron phases and TCE dechlorination." Environmental Science & Technology **38**(17): 4656-4663.

Tiraferri, A., K. L. Chen, R. Sethi and M. Elimelech (2008). "Reduced aggregation and sedimentation of zero-valent iron nanoparticles in the presence of guar gum." Journal of Colloid and Interface Science **324**(1-2): 71-79.

U.S.EPA. (2014). "Common chemicals found at superfund sites." Retrieved July 7th, 2014, from http://www.epa.gov/superfund/health/contaminants/radiation/chemicals.htm.

Vanstone, N., M. Elsner, G. Lacrampe-Couloume, S. Mabury and B. S. Lollar (2008). "Potential for identifyng abiotic chloroalkane degradation mechanisms using carbon isotopic fractionation." Environmental Science & Technology **42**(1): 126-132.

Varadachari, C., G. Goswami and K. Ghosh (2006). "Dissolution of Iron Oxides." Clay Research **25**: 1-19.

Wang, C. B. and W. X. Zhang (1997). "Synthesizing nanoscale iron particles for rapid and complete dechlorination of TCE and PCBs." Environmental Science & Technology **31**(7): 2154-2156.

Xie, Y. and D. M. Cwiertny (2010). "Use of Dithionite to Extend the Reactive Lifetime of Nanoscale Zero-Valent Iron Treatment Systems." Environmental Science & Technology **44**(22): 8649-8655.

Yan, W., A. A. Herzing, X.-q. Li, C. J. Kiely and W.-x. Zhang (2010). "Structural Evolution of Pd-Doped Nanoscale Zero-Valent Iron (nZVI) in Aqueous Media and Implications for Particle Aging and Reactivity." Environmental Science & Technology **44**(11): 4288-4294.

Yan, W., H.-L. Lien, B. E. Koel and W.-x. Zhang (2013). "Iron nanoparticles for environmental clean-up: recent developments and future outlook." Environmental Science: Processes & Impacts **15**(1): 63.

Yoon, S., D. S. Han, X. Liu, B. Batchelor and A. Abdel-Wahab (2014). "Degradation of 1,2-dichloroethane using advanced reduction processes." Journal of Environmental Chemical Engineering **2**(1): 731-737.

Yu, R., H. S. Peethambaram, R. W. Falta, M. F. Verce, J. K. Henderson, C. E. Bagwell, R. L. Brigmon and D. L. Freedman (2013). "Kinetics of 1,2-Dichloroethane and 1,2-Dibromoethane Biodegradation in Anaerobic Enrichment Cultures." Applied and Environmental Microbiology **79**(4): 1359-1367.

Zhang, W.-x. and D. W. Elliott (2006). "Applications of iron nanoparticles for groundwater remediation." Remediation Journal **16**(2): 7-21.

Zhong, L. S., J. S. Hu, H. P. Liang, A. M. Cao, W. G. Song and L. J. Wan (2006). "Self-Assembled 3D Flowerlike Iron Oxide Nanostructures and Their Application in Water Treatment." Advanced Materials **18**(18): 2426-2431.

Chapter 4

4. Conclusions

4.1 Summary and Conclusions

The current research work presents a novel approach for 1,2- DCA dechlorination using nanometals. This is the first nZVI-based formulation capable of abiotically dechlorinating 1,2-DCA. This treatment only requires dithionite as the main amendment for reactivity, decreasing the cost associated with adding a second noble metal as a catalyst. Though bare-nZVI was found to be more reactive than its stabilized counterpart, a stabilizer is recommended to enhance mobility during field application. It was shown that maintaining sulfidic conditions in solution has the potential of forming biphasic nanoparticles (Fe/FeS) and at the same time extending the reactive lifetime of nZVI. A dithionite formulation with other iron surfaces (i.e., iron sulfides and magnetite) also had significant reactivity towards 1,2-DCA. In the same way, a homogenous solution of dithionite was capable of degrading 1,2-DCA. However, use of dithionite as the main surface for reaction is recommended. Though it is currently unknown how an nZVI/dithionite formulation will react towards 1,2-DCA present in a mixture of contaminants, it is hypothesized that once dithionite is depleted, the nZVI remaining in solution will continue to react with other chlorinated compounds.

The main dechlorination product for 1,1,2-TCA dechlorination was vinyl chloride (VC). This product is consistent with β-elimination as the main reaction pathway.

4.2 Future Work

Future experiments and studies will involve:

1. Reactivity experiments with dichloromethane (DCM) as well as a solution containing multiple contaminants, (e.g., 1,2-DCA, DCM, 1,1,2-TCA, TCE). The successful dechlorination of 1,2-DCA suggest that other recalcitrant compounds might also be degradable with this treatment.
2. Studies on the product distribution and degradation pathways of 1,2-DCA by the nZVI/dithionite formulation.
3. Experiments with other iron and non-iron surfaces will also be tested. The aim is to further study the reactions of dithionite with these surfaces to determine what surface characteristics enhance the reactivity of the system.
4. Perform column experiments and settling tests to evaluate the mobility and stability of nZVI/dithionite nanoparticles.
5. Field application of an nZVI/dithionite treatment will be performed. Study on the reactivity, mobility and long term effect of dithionite on nZVI at the field scale will be studied.

Appendix A

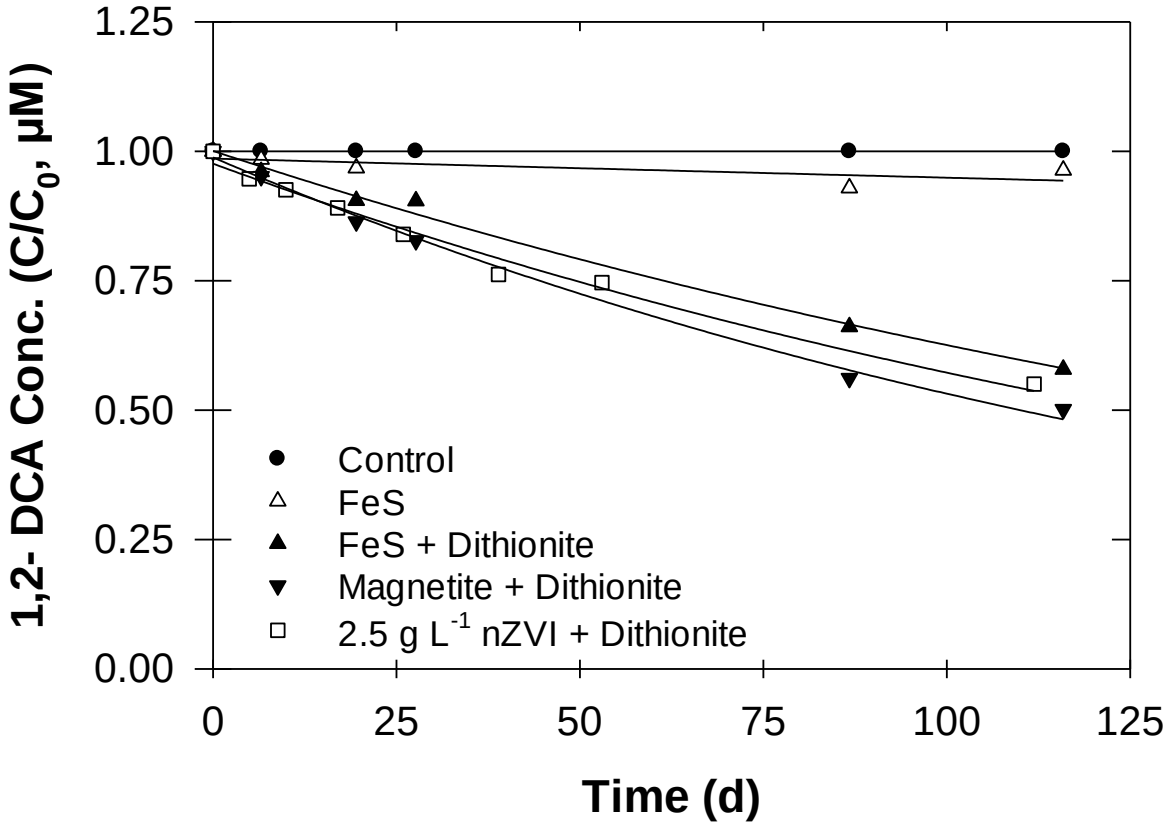

Figure A1 Effect of a two-fold decrease in nZVI concentration (2.5 g L^{-1}) and of two different iron surfaces (magnetite and iron sulfide) on 1,2-DCA dechlorination in the presence and absence of dithionite. Lines are pseudo-first order fittings of data points. Concentrations normalized to the initial concentration.

To account for losses in 1,2-DCA due to changes in the analytical method over the course of Exp.7, 8, 9 and 10, the percentage decrease of 1,2-DCA observed in the control at each sampling time was subtracted to the overall decrease of each individual experiment. This was done according to the following formula:

$\frac{C}{C_0} = \frac{C_{t-x}}{C_{0-x}} + (1 - \frac{C_{t-c}}{C_{0-c}})$, where:

C/C_0 = normalized concentration presented in Figure 1B

$C_{0\text{-}x}$ = initial concentration of Exp. 7, 8, 9 or 10

$C_{t\text{-}x}$ = concentration at time *t* of Exp. 7, 8, 9 or 10

$C_{0\text{-}c}$ = initial concentration of control

$C_{t\text{-}c}$ = concentration at time *t* of control

Percent degradation and k*obs* values presented in Table 3.1 were calculated from the normalized values shown in Figure A1.

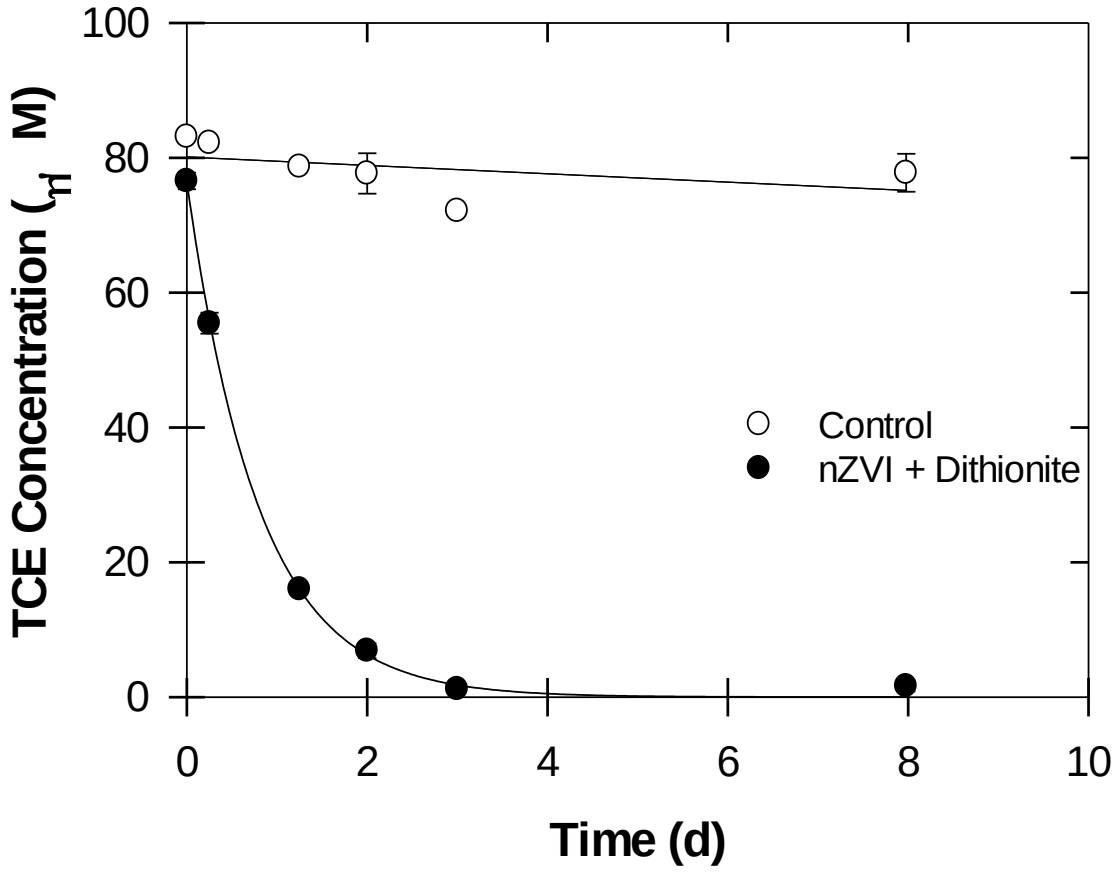

Figure A2 TCE Dechlorination by a 140 days old nZVI-Dithionite treatment: 5 g L^{-1} nZVI + 22 mM Dithionite. Lines are pseudo-first order fittings of data points. In some cases, error bars are smaller than the symbols.

Appendix B

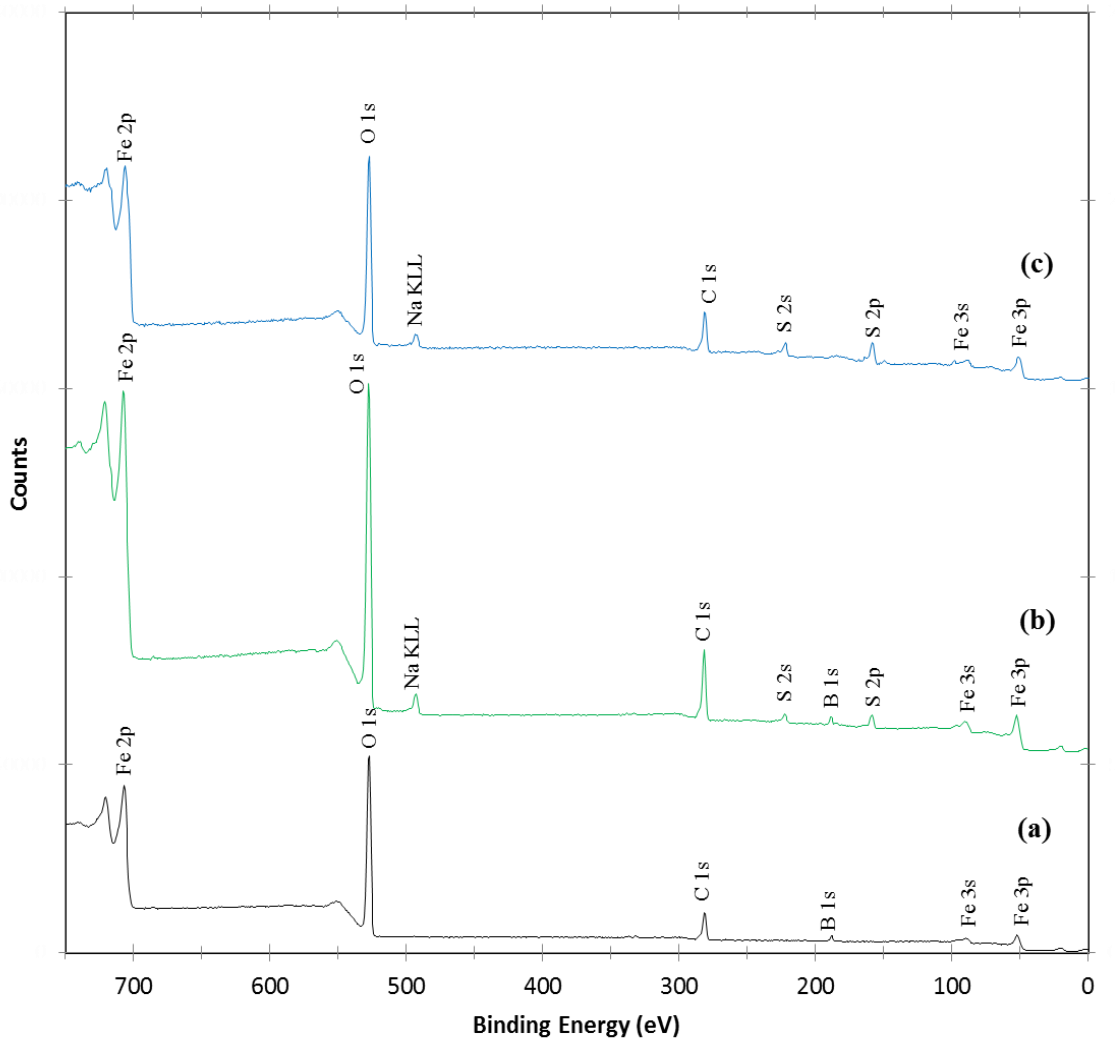

Figure B1 Wide-scan XPS spectra for: (a) Fresh nZVI; (b) Fresh nZVI + 22 mM Dithionite and (c) Old nZVI + 22 mM Dithionite.

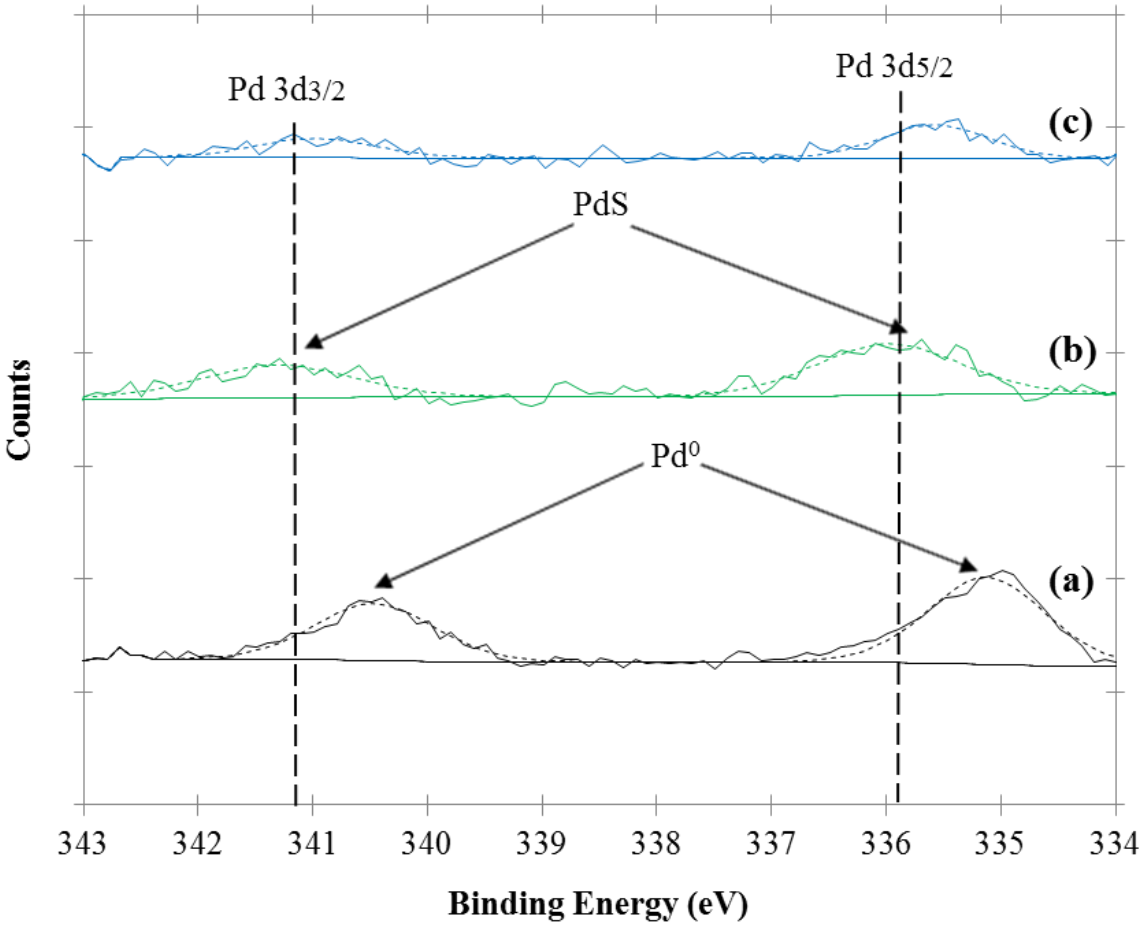

Figure B2 High resolution XPS spectra for Pd: (a) Fresh nZVI; (b) Fresh nZVI + Dithionite and (c) Old nZVI + Dithionite.

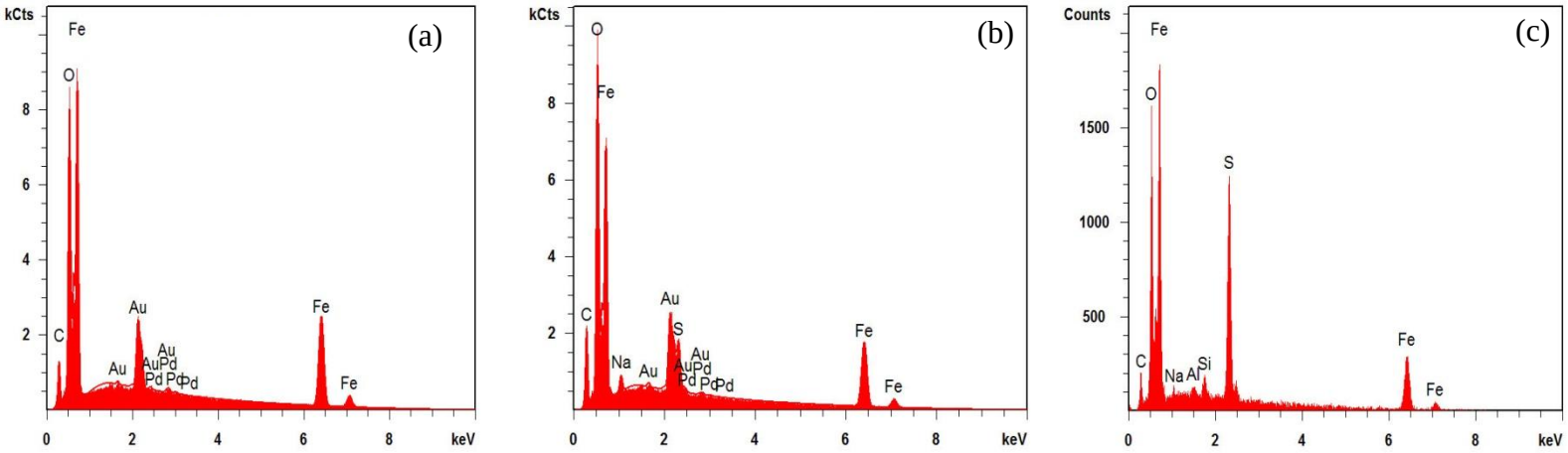

Figure B3 EDX analysis for: (a) Fresh nZVI; (b) Fresh nZVI + 22 mM Dithionite and (c) Old nZVI + 22 mM Dithionite.

Table B1 Particle surface composition determined by XPS (in atomic %)

Element	Fresh nZVI	Fresh nZVI + Dithionite	Old nZVI + Dithionite
Fe 2p	21	20.8	16.8
O 1s	50.8	44.3	43.4
S 2p	0	2.5	7
C 1s	21.7	24.2	26
Pd 3d	0.1	0	0.1
B 1s	6.4	5.8	2.1
Na 1s	N/A	2.4	3.4
Si 2p	N/A	N/A	1.2

Table B2 XPS Peaks for Palladium

Authors	Pd^0		PdS	
	$3d_{3/2}$	$3d_{5/2}$	$3d_{3/2}$	$3d_{5/2}$
This Study [a]	340.46	335.13	341.31	335.98
Matsumoto et al. (1980)	-	335.1 ±0.1	-	335.8 ±0.1
Muftikian et al. (1996)	340.3	335.0	-	-
Yan et al. (2010)	340.0	334.7	-	-

[a] Peaks for PdS taken from fresh nZVI-dithionite spectra

Table B3 EDX Weight Percentage

Element (wt %)	Fresh nZVI	Fresh nZVI + Dithionite	Old nZVI + Dithionite
Fe	80.57	65.31	60.58
O	13.2	19.17	17.87
S	N/A	2.71	12.7
C	5.53	11.6	7.35
Pd	0.7	0.34	N/A
Na	N/A	0.88	0.52
Si	N/A	N/A	0.79
Al	N/A	N/A	0.19

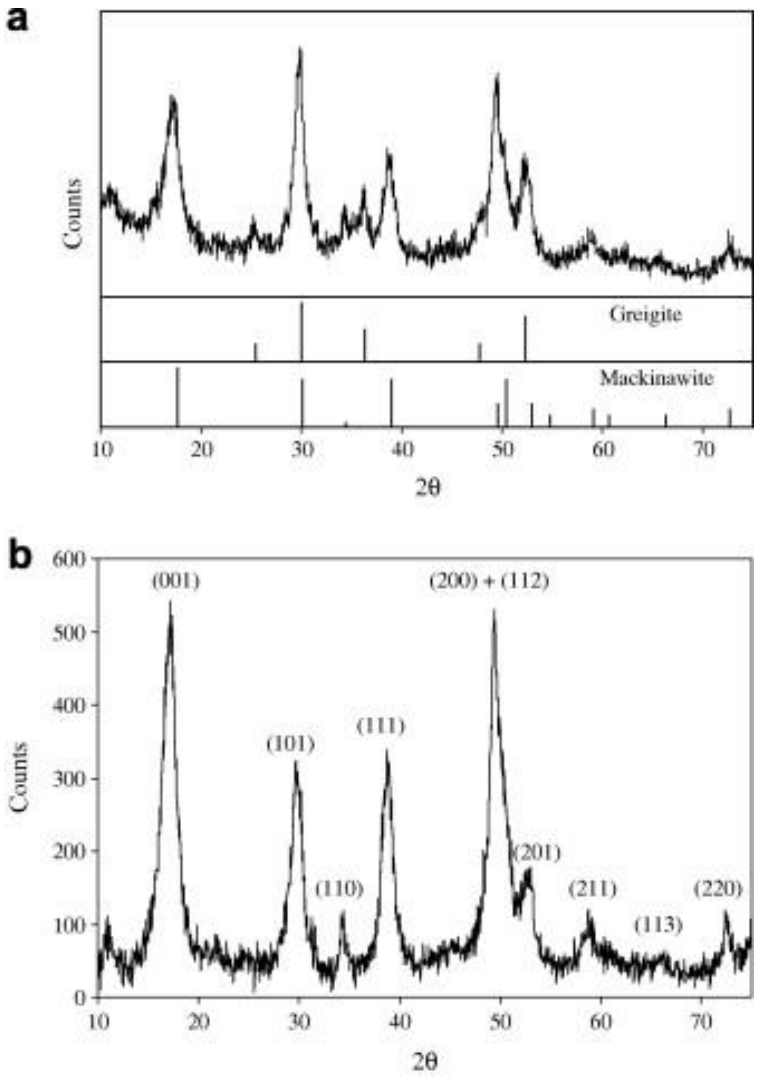

Figure B4 X-ray diffraction patterns for mackinawite. Cupper used as the radiation source (Jeong et al., 2008)

Curriculum Vitae

Name:	Ariel Nunez Garcia
Post-secondary Education and Degrees:	Utah State University 2007-2012 B.E.Sc
Related Work Experience:	Teaching Assistant The University of Western Ontario 2012-2014